ADVANCING PROSTATE CANCER THERAPY: SYNTHESIS AND CHARACTERIZATION OF DOCETAXEL-LOADED MAGNETIC IRON OXIDE NANOPARTICLES FOR CONTROLLED DRUG RELEASE

BY

CHISENGA IAN

A DISSERTATION SUBMITTED TO THE UNIVERSITY OF ZAMBIA IN PARTIAL FULFILMENT OF THE REQUIREMENTS FOR THE DEGREE OF

MASTER OF SCIENCE IN CHEMISTRY

THE UNIVERSITY OF ZAMBIA

LUSAKA

Copyright

Declaration

I, **CHISENGA IAN** hereby declare that this master's dissertation is my work and that the work contained herein is my own except where explicitly stated otherwise in the text, and that this work has not been submitted for any other degree, diploma, or other qualification at this or any other University.

Full Name: Chisenga Ian

Signature……  ……

Date:……01/06/2025……

Approval

This dissertation of Chisenga Ian is approved as a partial fulfilment of the requirements for the award of the degree of Master of Science in Chemistry by the University of Zambia.

Examiner's Name	Signature	Date
DR BAWES MYIRENDA		6/6/2025

Examiner I

Examiner's Name	Signature	Date
DR FRANCIS ICAYAMBA		06/06/2025

Examiner II

Examiner's Name	Signature	Date
DR. LUBINDA MUKOLOCO		06/06/2025

Examiner III

Examiner's Name	Signature	Date
Prof. R.O. Munyala		06/06/2025

Chairperson/Board of Examiners

Examiner's Name	Signature	Date
DR ONESMUS MUNYATI		06/06/2025

Supervisor

Abstract

Prostate cancer is one of the most common cancers among men worldwide, and current drug administration methods of front-line drugs like Docetaxel (DXL) face challenges, including non-specific treatment causing several side effects and the development of drug resistance, which affects patients' response and quality of life during treatment. Hence, there is a need for drug carriers such as Iron oxide nanoparticles, which are suitable for novel drug delivery systems due to low toxicity, biocompatibility, loading capacity, and controlled drug delivery to cancer cells. The purpose of the present study was to synthesize DXL-loaded pegylated magnetic Iron oxide nanoparticles (Fe_3O_4NPs) for controlled drug release in prostate cancer cells. In this study, Fe_3O_4NPs were synthesized by the co-precipitation, functionalized with folic acid (FA), loaded with DXL and encapsulated with polyethylene glycol (PEG). Structural analysis was done using ultraviolet-visible (UV-Vis) spectroscopy which showed changes in absorption spectra with each attached molecule a blue shift was observed due to particle size increase. X-ray diffraction (XRD) pattern showed that pure magnetite nanoparticles were synthesized. The Fourier Transform Infrared (FT-IR) results showed a peak at 583, 1089, and 1584 cm^{-1} these confirmed that Fe_3O_4 NPs were synthesized. The Langmuir adsorption isotherm model (R^2 =0.9947) was favoured over the Freundlich (R^2 =0.9441) and Temkin (R^2=0.8218). Drug release was faster at a potential of Hydrogen (pH) of 4.8 compared to pH 6.0, 7.0, and pH 7.45 with drug release percentage of 62.4%. 37.8%, 28.3%, and 24.0% respectively after 72 hr. Un-PEGylated Docetaxel-loaded nanoparticles showed a rapid drug release of about 98.8% after 7 hr. Drug release follows the Korsmeyer-Peppas kinetic model (R^2= 0.9949) via the Fickian release mechanism. This study showed that Docetaxel-loaded pegylated Fe_3O_4NPs could be beneficial for increasing the effect of anticancer drugs on cancer cells while minimizing side effects.

Dedication

This work is dedicated to my lovely family and friends.

Acknowledgments

I would like to offer my sincere gratitude to the Almighty God for all His blessings in my life. My sincere appreciation goes to my research supervisor, Dr. M.O. Munyati for his scholarly advice, guidance, and support that made the completion of this research easy. Many thanks to my co-supervisor Dr. Evelyn Funjika for her encouragement and leadership throughout my research project.

My thanks go to Dr. Mubanga Peter Cheuka for his leadership as coordinator of the postgraduate committee in the Department of Chemistry and for his guidance and support during my research work. Profound thanks also go to The University of Zambia, Departments of Chemistry (School of Natural Sciences), and Dr Phiri School of Mines for granting me access to the XRD instrument and Mr Mulunda Simoonga from Yash Life for the Fourier Transform -Infrared Spectrometric analysis.

I also want to thank my colleagues in the Material Science Research Group, Robert Singogo, Kaela Nonde, Happy Mabo, Isabel Chisulo, Lillia Mposha, Lameck Tembo, and Simon Mwale for their encouragement during my research period. I also thank Mr. Shadreck for his support in my research work.

I recognise the Department of Chemistry technical staff for their valued assistance and support.

I sincerely appreciate and acknowledge with thanks the International Science Programme (ISP) through the Sustainable Chemistry and Environment Programme (SCEP) at the University of Zambia for financial support.

I am truly thankful to my parents, Mr. Jimmy and Mrs. Leah Chisenga for their unwavering love and continued support throughout my life. I also thank my elder sister Eness C. Muchnga for her encouragement and guidance.

Finally, many thanks to my siblings and Yande Chisenga for being a formidable support system and motivation to have this project successfully done.

Table of Contents

List of Tables

List of Figures

List of Abbreviations

Abbreviations

AuNPs	Gold Nanoparticles
AFM	Atomic Force Microscope
DDS	Drug Development System
DLS	Dynamic Light Scattering
DNA	Deoxyribonucleic Acid
DOX	Doxorubicin
DXL	Docetaxel
EDC	N-Ethyl-N-(3-dimethylaminopropyl)Carbodiimide
FA	Folic Acid
FDA	Food Drug Administration
Fe_3O_4 NPs	Iron oxide nanoparticles
$FeCl_2 \cdot 4H_2O$	Iron dichloride tetrahydrate
$FeCl_3 \cdot 6H_2O$	Iron trichloride hexahydrate
FTIR	Fourier Transform Infrared
FWHM	Full Width at Half-Maximum
GLOBOCAN	Global Cancer Observatory
JCPDS	Joint Committee on Powder Diffraction Standards
MLNP	multilayered polymer nanoparticle
MNPs	Magnetic nanoparticles
NaOH	Sodium Hydroxide
NHS	N-Hydroxysuccinimide

PBS	Phosphate Buffer Solution
PEG	Poly-Ethylene Glycol
PEI	PolyEthylene Imine
pH	Hydrogen Potential
PSMA	Prostate-Specific Membrane Antigen
PTX	Paclitaxel
Q_{max}	Maximum Adsorption Capacity
RNAs	Ribonucleic Acids
SDGs	Sustainable Developmental Goals
SEM	Scanning Electron Microscope
siRNA	Small interfering Ribonucleic Acid
TEM	Transmission Electron Microscopy
THF	Tetrahydrofuran
UNZA	University of Zambia
UTH	University Teaching Hospital
UV-Vis	Ultraviolet Visible
XRD	X-ray diffraction

List of Symbols

Symbols

%T	Percent Transmittance
c	Centi
cm^{-1}	Per Centimetre
g	Gram, mass
h	hour
K_F	Freundlich constant
K_L	Langmuir constant
L	Litre, volume
m	Milli
mA	Milliamp
mL	Millilitre
n	Nano
ng/mL	Nano Gram Per Millilitre
^oC	Degrees Celsius
α	Alpha
β	Beta
θ	Theta (degree angle)
λ	Wavelength (nm)
μ	Micro
μL	Micro litre
π	Pi

Chapter One

Introduction

1.1 Background

Cancer is a major global health issue with the incidence of approximately 20 million new cases and 10 million deaths in 2022 globally (Bray et al., 2024). Prostate cancer is the second leading cause of death in men, particularly in developed countries. Globally, approximately 1.5 million new prostate cancer cases and 396,792 deaths were recorded in 2022, of which 863 deaths were recorded in Zambia (Ferlay et al., 2024). Researchers are working to improve the prevention, detection, and treatment of cancer to ensure survivors live longer and have better quality lives. Conventional cancer treatment methods include chemotherapy, immunotherapy, radiation therapy, and surgical resection (Debela et al., 2021). Among these, chemotherapy is the cheapest and most effective with a high patient compliance (Bekalu et al., 2023). However, these methods have a poor selection between normal and tumour cells, leading to reduced efficacy, drug resistance, increased toxicity, and difficulty in achieving optimal dosing (Banik, 2020, Rosenblum et al., 2018).

The development of drug delivery systems with controlled drug release is crucial in cancer chemotherapy to improve efficacy and reduce toxicity of anticancer drugs. Iron oxide nanoparticles have been recognized as promising platforms for drug delivery due to their magnetic properties and biocompatibility (Chen et al., 2018). The incorporation of drugs onto the surface of Fe_3O_4NPs can improve drug efficacy by increasing and maintaining drug concentration at the target site (Fernandes, 2023). Controlled drug release from Fe_3O_4NPs can overcome the limitations of conventional chemotherapy, such as poor bioavailability and drug resistance (Li et al., 2019).

Functionalized iron oxide nanoparticles can be conjugated with various biomolecules such as antibodies, peptides, and nucleic acids to target specific cells or tissues, making them ideal for targeted drug delivery (Sachdeva et al., 2022). Though widely used for prostate cancer treatment, DXL effectiveness is limited by its poor solubility and toxicity to healthy cells (Al Saqr et al., 2021). Therefore, controlled release of DXL using functionalized pegylated iron oxide nanoparticles can enhance its efficacy and reduce toxicity.

Docetaxel is a semisynthetic anticancer mitotic ("antineoplastic" or "cytotoxic") chemotherapy drug in the *taxoid* family. It is derived from the European yew tree (*Texus baccata*). The DXL is recommended for optional treatment in cancer patients with hormone-refractory metastatic prostate cancer (Rivero-Buceta et al., 2019, Markowski and Carducci, 2017, Alken and Kelly, 2013). It is a chemotherapeutic medication against a wide range of solid tumours, including lung, breast, head, prostate, neck, and ovarian cancers (de Oliveira et al., 2013). Many researchers have established that DXL binds to β-tubulin, which interferes with the normal function of the microtubule polymerization dynamics, dividing cell mitosis, interface microtubule function, and triggering apoptosis (Kraus et al., 2003). Low water solubility, severe allergic reactions, and systemic toxicity are among DXL limitations (Park et al., 2014). To overcome these drawbacks of DXL in clinical use, nano-based drug delivery systems like liposomes, inorganic nanoparticles, magnetic nanoparticles, polymeric nanoconjugates, and nanotubes have been formulated for DXL delivery (Thambiraj et al., 2019, Sato et al., 2013, Hua et al., 2017).

Recent studies have shown the potential of drug-loaded Fe_3O_4NPs for prostate cancer treatment. The use of stimuli-responsive materials and targeting ligands can enhance the specificity and selectivity of drug delivery to prostate cancer cells (Zhang et al., 2022, Zhou et al., 2017). The use of drug-loaded Fe_3O_4NPs for controlled drug release can improve treatment outcomes, reduce toxicity, and enhance patient quality of life. This research therefore seeks to design a drug-loaded nano drug delivery system that will enhance controlled drug release and establish the drug release kinetics.

In this research, we investigated the use of functionalized iron oxide nanoparticles for the controlled release of DXL in vitro intended for future application prostate cancer therapy. We synthesized iron oxide nanoparticles with a diameter of 10-20 nm and functionalized their surface with folic acid (FA). The nanoparticles were loaded with DXL and encapsulated with PEG for increased stability then characterized using various techniques such as XRD, for morphology and size. Chemical structure and properties analysis was conducted using FTIR, and UV-VIS, also the Iron oxide nanoparticles were subjected to re-binding experiments to investigate their adsorption characteristics. Lastly, drug release of unPEGylated and PEGylated DXL-loaded Fe_3O_4 NPs, was carried out. The PEGylated DXL-loaded Fe_3O_4 NPs showed a steady drug release pattern compared to the unPEGylated one.

Overall, our findings suggest that functionalized iron oxide nanoparticles could be a promising platform for controlled drug release in prostate cancer therapy, with the potential to enhance the drug bioavailability in prostate cancer cells compared to the normal prostate cells, which then increases efficacy and reduces the toxicity of chemotherapy drugs like DXL. The release kinetics favoured the Korsmeyer-Peppas model, and the Fickian release mechanism was followed.

1.2 Statement of the Problem

Chemotherapy remains the most used treatment method for cancers such as prostate cancer and drugs like DXL are used for most cancers. Although DXL has significant anti-cancer effects, its use is limited due to systemic side effects like hepatotoxicity (Pieniążek et al., 2013), nephrotoxicity (Baş and Nazıroğlu, 2019) and Neutropenia (Ho and Mackey, 2014) in many patients. These side effects result from the non-specific distribution of chemotherapeutic agents, which damage both cancerous and healthy cells due to the lack of targeted delivery mechanisms. This leads to reduced efficacy due to fluctuating drug concentration to exert a therapeutic effect, development of drug resistance (Wang et al., 2019) and difficulty in achieving optimal dosing (Khalid et al., 2017). Therefore, leveraging on the pH differences of cancer and the normal cells' microenvironment, a nano-drug delivery system that would differentially deliver DXL to the tumour cells and release them in a controlled manner is urgently needed.

1.3 Significance of the Study

Zambia continues to face a high burden of cancer-related morbidity and mortality. The 2022 GLOBOCAN report estimated that the overall age-standardized cancer incidence rate for both sexes in Zambia was 159.5 per 100,000 (15, 296 cases) for all cancers. They also estimated the age-standardized mortality rate to be 109.2 per 100,000 (9, 770 deaths), which means that the majority (~63.8%) of new cancer cases in Zambia die from the disease (Ferlay et al., 2024). Although potent drugs like Docetaxel are available, the current method of drug administration results in poor selection between normal and tumour cells, leading to side effects and lower therapeutic benefit. This study can potentially reduce side effects associated with anticancer drugs and maintain drug concentration by controlled drug release. The study aligns with Sustainable Developmental Goal 3, which is to promote good health and well-being (SDGs), which in turn will enable the achievement of other SDGs.

1.4 Objectives of the Study

1.4.1 Main objective.

The study aims to design, synthesise and characterise Docetaxel-loaded magnetic iron oxide nanoparticles (Fe_3O_4NPs) for controlled drug release and investigate the drug release kinetics under varying pH conditions.

1.4.2 Specific Objectives.

(i) To design, synthesise and characterise Docetaxel-loaded pegylated magnetic iron oxide nanoparticles (Fe_3O_4@FA@DXL@PEG)
(ii) To investigate the effect of pH on drug release profiles
(iii) To analyse drug release kinetics

1.5 Research questions.

(i) How can Docetaxel-loaded Pegylated Magnetic iron oxide nanoparticles be synthesized and characterised?
(ii) What is the effect of pH on the drug release profiles of the developed Docetaxel-loaded pegylated magnetic iron oxide nanoparticles?
(iii) What drug release kinetic model and mechanism is being followed?

Chapter Two

Theoretical Background

2.1 Introduction

This chapter discusses an overview of drug delivery systems, magnetic nanoparticles, current prostate cancer drugs, targeted drug delivery, and the application of magnet nanoparticles in drug delivery. The discussion will also briefly outline the classifications, and the pros and cons associated with each type.

2.2 Drug Delivery Systems (DDS)

Drug delivery systems play a crucial role in modern medicine, enabling efficient and targeted delivery of therapeutic agents to specific sites within the body (Tewabe et al., 2021). These systems have evolved significantly over the years (Adepu and Ramakrishna, 2021), offering various types of delivery mechanisms that differ in their advantages and disadvantages. Here is an overview of different drug delivery systems, their classifications.

2.3 Types of Nanoparticles used for Docetaxel Delivery

Nanoparticles (NPs) represent a particularly smart drug delivery approach for drug delivery for several reasons, including composition, structure, and surface characteristics. The NP composition can be widely varied, which allows the carriers to be modified for specific applications and target specificity (Mitchell et al., 2021). Polymeric, lipid-based, and inorganic NPs are the most used for targeted drug delivery. NP-based drug delivery systems can be classified into different types, including polymeric, inorganic, and lipid-based vehicles.

2.3.1 Polymeric Nanoparticles

Polymeric Nanoparticles (NPs) can be synthesised using natural or synthetic materials and form various possible structures and can be sub-categorised as shown (Figure 1). Polymer NPs are synthesised using a range of methods, including emulsification (Brown et al., 2020), ionic gelation, nano-precipitation (Zhang et al., 2019, Le et al., 2018), and microfluidics (Zhang et al., 2020). Polymer NPs also have variable drug delivery capabilities which depend on where and how they combine with the drugs, for example, drugs can be bonded to the NP's surface, embedded into the polymer matrix, encapsulated within the NP's nucleus, or bound to the polymer through chemical reactions (Guo et al., 2022). Polymer NPs are an ideal material for

drug co-delivery. The loaded drugs can be hydrophilic and hydrophobic compounds or other small molecules and biological macromolecules, such as RNAs/DNAs, proteins, and anticancer drugs like Docetaxel. Moreover, biocompatible polymers used for drug delivery are often biodegradable and have non-harmful by-products, such as non-toxic alcohols, acids, and other relatively easily eliminated products (Senapati et al., 2018). These by-products can then contribute to drug release properties as a result of their erosion/degradation, not to mention drug diffusion through polymeric material. By regulating the chemical and physical properties of NPs, we can realize accurate control of drug loading effect and release kinetics. However, the disadvantages of polymeric NPs include an increased risk of particle aggregation and toxicity (Zielińska et al., 2020).

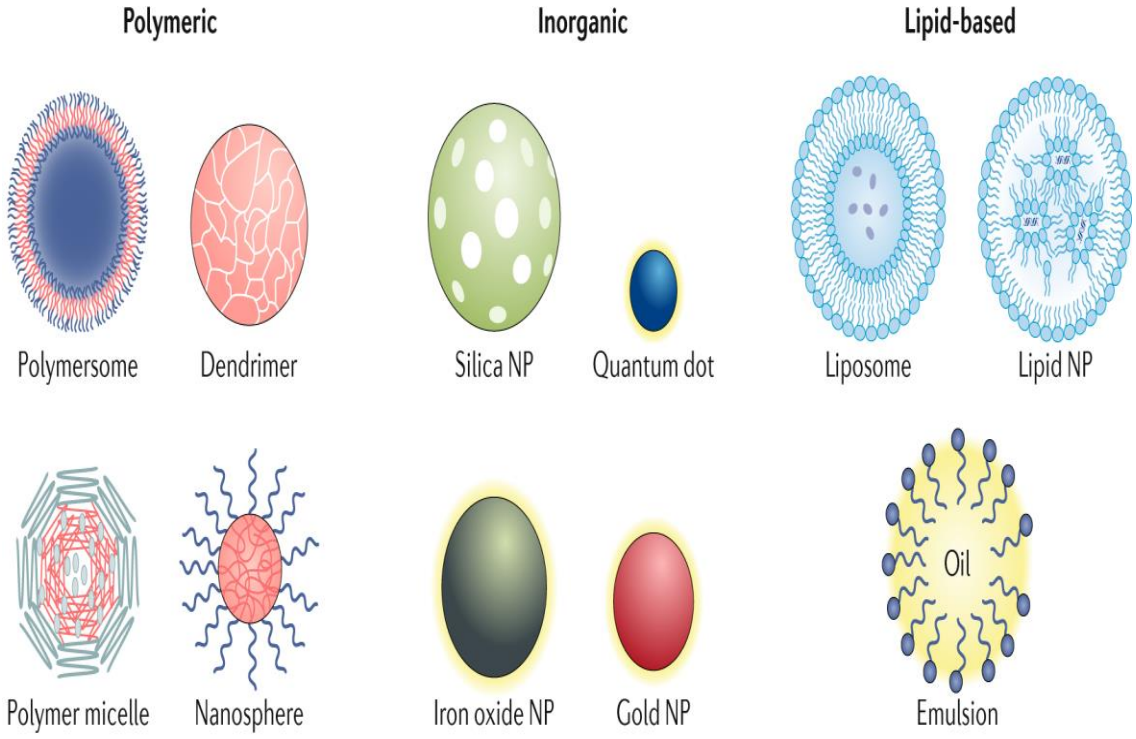

Figure 1: Different types of nanoparticles are used for Drug (Mitchell et al., 2021).

2.3.2 Lipid-based NPs

Lipid-based NPs are mostly spherical platforms comprising at least one lipid bilayer surrounding at least one internal aqueous compartment (Figure 1). As a delivery system, lipid-based NPs offer many advantages including simplicity of formulation, self-assembly, high bioavailability, biocompatibility, ability to carry large payloads and a range of physicochemical

properties that can be controlled to modulate their biological characteristics (Fonseca-Santos et al., 2015, Sercombe et al., 2015). For these reasons, lipid-based NPs are the most common class of FDA-approved nanomedicines (Fenton et al., 2018). Though they have a low encapsulating efficiency (Mitchell et al., 2021).

2.3.3 Inorganic NPs

The inorganic nanomaterials are designed into various structures, geometries, and sizes as shown (Figure 1). These types of inorganic NPs have unique magnetic, radioactive, and plasmonic properties, which make them qualified for clinical diagnosis, imaging, and photothermal therapy. Most of them have good biocompatibility and stability. Among them, gold nanoparticles (AuNPs) are the most frequently studied with their different form like nanospheres and nanorods, nanoshells (Yang et al., 2019b). Additionally, the unique magnetic, electrical, and optical nature of inorganic NPs such as Au NPs, quantum dots (Wagner et al., 2019), and iron oxide, decided by the substrate properties, providing them with many potential effects, like photo-thermal transforming effect to be a promising application for thermal-therapy.

Iron oxide is a common inorganic NP, it consists of Fe_3O_4 or Fe_2O_3 with superparamagnetic properties in some sizes and has been successfully applied in contrast agents, drug delivery carriers, and therapy. The NPs account for the vast majority of clinical studies in the world, including prognostic imaging and nano-based radiotherapy for metabolic diseases and cancers. Calcium phosphate and mesoporous silica are the other important inorganic NPs used to transport DNA/RNA or drugs (Mitchell et al., 2021). These metal cores of NPs have been shown in cell and animal tests to exhibit extremely low cytotoxicity and to maintain a stable state during ingestion and organ targeting with few interactions with the environment (Yang et al., 2021). Also, effort should be made to promote the solubility and reduce the toxicity of these materials, especially by reducing the heavy metals in the preparation system.

2.4 Magnetic Nanoparticles

Magnetic nanoparticles (MNPs) have emerged as a versatile platform for targeted drug delivery due to their unique magnetic properties and controllable surface chemistry (Smith et al., 2006). These nanoparticles, typically ranging from 1 to 100 nanometers in size, can be engineered using various synthesis methods to achieve desired characteristics (Chen et al., 2018). By functionalizing the surface of MNPs with biomolecules such as polymers or antibodies, their

stability, biocompatibility, and targeting capabilities can be significantly enhanced (Yin et al., 2015). The key advantage of MNPs lies in their responsiveness to external magnetic fields, which allows for precise manipulation and targeting within the body. Upon reaching the target site, controlled drug release can be achieved through stimuli-responsive mechanisms, such as changes in pH, temperature, or the application of an alternating magnetic field (Eslami et al., 2022). This combination of magnetic guidance and controlled release offers great potential for improving drug delivery efficacy while minimizing off-target (Sutradhar and Amin, 2014).

Chapter Three

Literature Review

3.1 Introduction

Prostate cancer is the second most common cancer in men. It is a kind of cancer that starts in the prostate, a small walnut-shaped gland in males that produces seminal fluid. In the last two decades, chemotherapy has come to play a vital role in prostate cancer treatment (Rawla, 2019). Docetaxel is a widely used chemotherapy drug in the treatment of various malignancies, including breast, lung, and prostate cancer (Sousa-Pimenta et al., 2023). Approved by the FDA in 2004, Docetaxel has revolutionized the treatment landscape for prostate cancer, significantly extending survival and improving the quality of life for many patients.

In this literature review, we aim to provide an overview of prostate cancer chemotherapy, identified challenges and recent research on the use of functionalized nanoparticles for the controlled release of drugs in cancer treatment, with a considerable focus on synthesis, characterization, drug loading, drug release, toxicity, and drug release kinetics. We also establish potential areas for future researchers.

3.2 Side Effects of Docetaxel Therapy.

While DXL has shown efficacy in controlling tumour growth and improving patient outcomes, it is also associated with a range of side effects and challenges that can impact patient quality of life and its future administration. These side effects include Neutropenia; a decrease in white blood cell count. This increases the susceptibility of the patient to infections, hence, patients may require treatment with antibiotics and dose adjustments of docetaxel (Zhuang and Kang, 2018). The other is Bone Marrow Suppression: Docetaxel is associated with the suppression of bone marrow function, leading to a decrease in red blood cells (anaemia) and platelets (thrombocytopenia). This has the potential to increase the risk of fatigue, bruising, and bleeding (Sousa-Pimenta et al., 2023) also Alopecia is the most frequent cosmetic side effect of docetaxel therapy. Patients experiencing hair loss may have severe psychological effects that alter their perception of their bodies and sense of self (Ho and Mackey, 2014).

3.3 Limitations of Conventional Docetaxel Therapy

Apart from the few cited side effects, several limitations characterized the conventional administration of Docetaxel. Some of the limitations are discussed briefly in the sections that follow.

3.4 Drug Resistance and Reduced Efficacy

Docetaxel remains a cornerstone of treatment, especially for advanced prostate cancer. However, the emergence of resistance to docetaxel presents a significant challenge in the management of prostate cancer patients. According to a study by Sekino and Jun (2020), specific genetic alterations are associated with resistance, also mutations impacting drug metabolism, DNA repair, cell survival pathways, cell cycle regulation, and the androgen receptor (AR) signaling pathway may be responsible for resistance to docetaxel thus leads to reduced efficacy. Furthermore, the research elucidated how prostate cancer cells activate survival mechanisms, such as the upregulation of anti-apoptotic proteins or activation of signaling pathways like PI3K/Akt, to evade the cytotoxic effects of docetaxel and other treatments (Sekino and Teishima, 2020). Expanding on this, Lima et al (2021) established drug-resistant prostate cancer cell lines and identified several mechanisms that may be associated with the development of drug resistance in prostate cancer. Their findings underscore the complexity of docetaxel resistance and highlight the need for multifaceted therapeutic approaches to effectively target resistant prostate cancer cells (Lima et al., 2021).

Additionally, the genetic landscape of small-cell neuroendocrine prostate cancer (SCNPC), a highly aggressive subtype linked to treatment resistance, was investigated by Aggarwal et al. (2019). They discovered genetic changes in genes related to DNA repair, neuroendocrine differentiation, and cell cycle regulation that may be responsible for SCNPC patients' resistance to docetaxel and other treatments (Aggarwal et al., 2018). Recently, Dong et al. (2018), study demonstrated that MALAT1 promotes docetaxel resistance by sponging miR-145-5p,5-5p, thereby upregulating its target gene AKAP12. These findings provide mechanistic insights into the involvement of MALAT1 and the miR-145-5p/AKAP12 axis in docetaxel resistance, suggesting potential therapeutic targets for overcoming resistance in prostate cancer patients (Xue et al., 2018). These investigations have brought to light the intricate interactions amongst noncoding RNA, tumour microenvironment, and genetic modifications that mediate resistance

to chemotherapy based on docetaxel, demonstrating why new treatment approaches are required to overcome docetaxel resistance and enhance the prognosis of individuals with prostate cancer and increase the drug efficacy.

3.5 Dosing Optimization and Drug Stability

Docetaxel dosage optimization presents several difficulties, particularly in balancing therapeutic efficacy with tolerability and minimizing the risk of toxicity. Through the combination of pharmacogenomics, pharmacokinetics, and pharmacodynamics, a study by Papachristo et al. (2023) highlighted the rising role of pharmacogenomics, pharmacokinetics, and pharmacodynamics in exploring the evolving landscape of dose optimization in oncology. To enhance drug efficacy while avoiding toxicity, it emphasizes the significance of customized dosage regimens based on genetic variants, drug metabolism profiles, and tumour features. They emphasized the necessity of using precision dosage techniques to maximize the benefits of docetaxel therapy while reducing side effects. Examples of these techniques include therapeutic drug monitoring, pharmacogenetic testing and the use of drug delivery systems (Papachristos et al., 2023).

Furthermore, drug stability presents a significant challenge in the formulation and administration of docetaxel, particularly regarding its aqueous solubility and susceptibility to degradation. Research has investigated several ways to formulate docetaxel to improve its stability and bioavailability. Li et al. (2020), for instance, explored the creation of formulations based on nanoparticles for better drug delivery and stability in their work. They discussed the advantages of nanoparticle formulations, such as improved solubility, controlled release, and reduced systemic toxicity, in enhancing the stability and therapeutic efficacy of docetaxel. Their work points to the need for nanoparticle incorporation in drug delivery for improved stability (Li et al., 2019, Liu et al., 2018).

3.6 Fluctuating drug concentration and bioavailability

In prostate cancer treatment using Docetaxel, fluctuating drug concentrations can significantly impact therapeutic outcomes because chemotherapeutic agents like Docetaxel relies on consistent and adequate exposure to exert cytotoxic effects on cancer cells. Fluctuating Docetaxel concentrations may result in periods of subtherapeutic dosing, where the drug levels fall below the effective range needed to inhibit cancer cell growth effectively. This suboptimal

exposure can lead to reduced treatment responses, including slower tumour regression, shorter durations of disease control, and lower overall survival rates in prostate cancer patients. It also has the potential to contribute to the development of drug resistance in prostate cancer cells, where cancer cells survive and proliferate despite treatment, ultimately leading to treatment failure and disease progression.

Furthermore, fluctuations in Docetaxel concentrations can also lead to periods of drug overexposure, resulting in increased toxicity and adverse effects impacting patient quality of life and treatment adherence, also affects drug bioavailability, influencing the extent and rate at which Docetaxel is absorbed, distributed, metabolized, and eliminated from the body impacting the overall pharmacokinetic profile of Docetaxel and its therapeutic effectiveness. Therefore, maintaining stable and optimal Docetaxel concentrations is essential for maximizing treatment efficacy and minimizing toxicity in prostate cancer patients.

Therefore, addressing the challenges of systemic toxicity, drug resistance, dosing optimization and drug stability of docetaxel requires a multidisciplinary, among the recommendations is the use of drug delivery systems with improved stability that will release docetaxel in a controlled manner to maintain drug concentration within the therapeutic threshold, enhance its drug efficacy while reducing the side effect.

Cancer treatment is a challenging and complex process that requires controlled drug delivery and release to the affected cells while minimizing the effect on healthy cells. Recently nanoparticles have gained significant attention in cancer therapy due to their potential as drug delivery systems, they are being extensively studied in cancer therapy due to their unique properties such as small size, high surface area-to-volume ratio, and ability to carry drugs (Liu et al., 2016). Apart from that their improved drug solubility, targeted drug delivery, and reduced systemic toxicity make them a promising strategy for controlled drug release in cancer treatment.

3.7 Docetaxel Delivery Using Functionalized Iron Oxide Nanoparticles

The development of effective drug delivery systems has been a focal point in enhancing treatment efficacy while minimizing adverse effects. Docetaxel, a potent anticancer agent, has shown promising results in combating various malignancies (Tas and Keklikcioglu Cakmak, 2021). However, its clinical utility is often hindered by poor solubility, and systemic toxicity

(Cheng et al., 2021). Addressing these challenges, researchers have turned to nanotechnology to devise innovative drug delivery strategies. Among these, functionalized iron oxide nanoparticles have emerged as a promising platform for docetaxel delivery. Iron oxide nanoparticles possess inherent magnetic properties and exhibit excellent biocompatibility, making them suitable candidates for biomedical applications (Montiel Schneider et al., 2022). Their small size facilitates cellular uptake and intracellular trafficking, crucial for drug delivery. Additionally, Fe_3O_4NPs can be easily functionalized with various molecules, enabling targeted drug delivery and controlled release (Song et al., 2019).

3.8 Synthesis Methods for Fe_3O_4NPs

In recent years, various methods have been developed for the synthesis of functionalized nanoparticles, including physical methods such as laser ablation and chemical methods such as co-precipitation, sol-gel, and hydrothermal methods (Li et al., 2019). In 2010, Li et al. reported the synthesis of chitosan nanoparticles for the controlled release of doxorubicin, a common chemotherapy drug used in cancer treatment while Wang et al. reported the successful synthesis of doxorubicin-loaded magnetic nanoparticles functionalized with a folate receptor-targeting ligand. They demonstrated enhanced cellular uptake and cytotoxicity against folate receptor-overexpressing cancer cells compared to non-functionalized nanoparticles (Wang et al., 2019).

In another study, Liu et al. synthesized folate-conjugated chitosan nanoparticles loaded with Doxorubicin (DOX) (Liu et al., 2018). The folate-conjugated chitosan nanoparticles showed enhanced cellular uptake and cytotoxicity against folate receptor-overexpressing cancer cells compared to non-targeted chitosan nanoparticles. Furthermore, the folate-conjugated chitosan nanoparticles exhibited prolonged drug release and improved therapeutic efficacy in a xenograft tumour model. Recently Singogo reported the synthesis of Iron Oxide nanoparticles by co-precipitation, he reported that it is a simple and cheaper method that uses pH for size control and magnetic strength. He reported that the Atomic Force Microscope (AFM) image showed clear small spherical nanoparticles with an overall average size of 82.7 nm (Singogo, 2022).

3.9 Characterization of Functionalized Fe_3O_4NPs for Docetaxel Delivery

The characterization of functionalized nanoparticles is essential to determine their size, shape, surface charge, drug loading, and targeting efficiency. Various techniques such as

Transmission Electron Microscopy (TEM), XRD, and UV-Vis spectroscopy. Dynamic Light Scattering (DLS), zeta potential measurement, and FTIR have been used for nanoparticle characterization (Chen et al., 2018). TEM is a powerful tool for visualizing nanoparticles, as it can provide information on their size, shape, and distribution. DLS is used to measure the hydrodynamic diameter of the nanoparticles in solution, which can provide information on their stability and aggregation behaviour (Ansari et al., 2019). FTIR and UV-Vis have been used for chemical structure and properties analysis. Zeta potential measurement is used to determine the surface charge of the nanoparticles, which can affect their stability and cellular uptake. UV-Vis spectroscopy is also used to determine the drug loading efficiency and release profile of the nanoparticles (Lourenço et al., 2019). The synthesis and characterization of functionalized nanoparticles for drug delivery in cancer treatment have been extensively studied. Emulsion-based methods, chemical conjugation, and physical adsorption have been used to synthesize functionalized nanoparticles, and TEM, DLS, zeta potential measurement, and UV-Vis spectroscopy have been used to characterize them.

3.10 Drug Loading

Drug loading of anticancer drugs on functionalized nanoparticles for drug delivery in cancer treatment is an area of active research that has shown significant promise in improving the therapeutic efficacy and specificity of chemotherapy. By loading anticancer drugs onto functionalized nanoparticles, drug delivery can be targeted specifically to cancer cells, reducing off-target effects and improving the efficacy of treatment (Tas and Keklikcioglu Cakmak, 2021). It is a crucial step in nanoparticle-based drug delivery systems. Various factors such as the type of drug, nanoparticle size, and surface chemistry, affect drug loading efficiency (Herdiana et al., 2024, Attia et al., 2022).

There are various methods available for loading drugs onto functionalized nanoparticles for drug delivery in cancer treatment, each with its advantages and limitations (Hu et al., 2011). One method is adsorption, which could be physical or chemical adsorption. Physical adsorption involves physically adsorbing the drug onto the surface of the nanoparticles through electrostatic or hydrophobic interactions. It is a simple, low cost, and has a high drug loading capacity, but may result in rapid drug release (Gao et al., 2020).

While chemical adsorption (Covalent conjugation) is a method that chemically attaches the drug to the surface of the nanoparticles through covalent bonds. This method provides stable

drug loading and controlled release and can improve the specificity and selectivity of drug delivery. However, the conjugation process can be complex and time-consuming and may result in reduced drug loading capacity (Fasiku et al., 2020).

Encapsulation is another method that involves incorporating the drug into the interior of the nanoparticles through solvent evaporation or emulsion techniques. Encapsulation provides sustained release of the drug, protecting it from degradation and reducing off-target effects. However, encapsulation can be challenging for some drugs, and the drug loading capacity may be limited (Adepu and Ramakrishna, 2021).

Physical entrapment involves physically trapping the drug within the matrix of the nanoparticles, typically through nano-precipitation or coacervation techniques. Physical entrapment provides sustained release and high drug-loading capacity but may result in incomplete drug release and limited drug stability (Adepu and Ramakrishna, 2021). In addition to these methods, the size, shape, and surface chemistry of the nanoparticles, as well as the physicochemical properties of the drug, can influence drug loading efficiency and efficacy (Banerjee et al., 2016). Therefore, selecting an appropriate drug loading method and optimizing the drug-nanoparticle system is critical for achieving effective drug delivery in cancer treatment.

Overall, the selection of a drug-loading method for functionalized nanoparticles should be based on the specific drug, the desired release profile, and the characteristics of the nanoparticle system. Recent advancements in nanoparticle synthesis and characterization have enabled the development of more sophisticated drug delivery systems with improved drug-loading efficiency and therapeutic efficacy (Patra et al., 2018).

Several studies have reported successful drug loading of functionalized nanoparticles for cancer treatment. For instance, (Li et al., 2019), reported the successful loading of paclitaxel (PTX) onto folic acid-functionalized silica nanoparticles (FA-SiO_2 NPs) with high drug loading efficiency. Another study investigated the use of a biocompatible and biodegradable polymeric nanoparticle system for drug delivery of paclitaxel, an anticancer drug used to treat various types of cancer, including breast, ovarian, and lung cancer (Yao et al., 2020). The nanoparticles were functionalized with a targeting ligand, hyaluronic acid, to enhance their uptake by cancer cells. The results showed that the drug-loaded nanoparticles had high encapsulation efficiency

and sustained drug release, with a significant reduction in the viability of cancer cells in vitro (Patra et al., 2018).

In another study, Liu and colleagues developed a drug delivery system based on mesoporous silica nanoparticles functionalized with polyethyleneimine (PEI) and loaded with paclitaxel. The functionalized nanoparticles exhibited improved cellular uptake and enhanced anticancer efficacy compared to free paclitaxel. The authors suggested that the improved efficacy may be attributed to the increased cellular uptake of the nanoparticles through electrostatic interactions between the PEI and the cancer cell membrane (Liu et al., 2018). Folate receptor-targeted chitosan nanoparticles have also been investigated as a drug delivery system for doxorubicin, a commonly used anticancer drug (Zhang and Zhang, 2013). The results showed that the drug-loaded nanoparticles had a high drug-loading capacity and sustained release, leading to increased cytotoxicity against cancer cells in vitro. The folate receptor-targeted nanoparticles also exhibited enhanced cellular uptake compared to non-targeted nanoparticles.

In addition to targeting ligands, the physicochemical properties of the nanoparticles can also influence their drug loading and delivery efficacy. A study by Carvalho investigated the use of dynamic light scattering (DLS) as a tool for characterizing PEGylated drug delivery systems. The authors demonstrated that DLS could be used to determine the size, polydispersity index, and zeta potential of the nanoparticles, which are important parameters that can influence drug loading and delivery efficacy (Carvalho et al., 2018).

Drug loading of anticancer drugs onto functionalized nanoparticles for drug delivery in cancer treatment is a promising area of research that has the potential to improve the therapeutic efficacy and specificity of chemotherapy. The incorporation of targeting ligands can enhance the cellular uptake and cytotoxicity of the nanoparticles, and sustained drug release can lead to improved therapeutic efficacy. Further studies are needed to optimize the design and synthesis of functionalized nanoparticles for drug delivery in cancer treatment, including investigations into the physicochemical properties of the nanoparticles that can influence drug loading and delivery efficacy.

3.11 Controlled Drug Release:

Controlled drug release from functionalized nanoparticles is a crucial aspect of drug delivery in cancer treatment. It allows for sustained and targeted release of anticancer drugs to the

tumour site, improving efficacy and reducing off-target effects. Various approaches have been developed to achieve controlled drug release from functionalized nanoparticles, each with its advantages and limitations (Mi et al., 2022). Controlled drug release is a critical aspect of nanoparticle-based drug delivery systems. There are various factors such as nanoparticle size, surface chemistry, and drug properties that affect drug release kinetics. Several studies have reported the successful controlled release of drugs from functionalized nanoparticles for cancer treatment. For instance, Liu et al reported the sustained release of doxorubicin (DOX) from polyethylene glycol (PEG)-coated gold nanoparticles (AuNPs) over 48 hours (Liu et al., 2019). One approach is based on stimuli-responsive materials, such as pH-sensitive polymers, that can release the drug in response to changes in the local environment. Compared to normal cells, cancer cells have unique pH, a characteristic that has been investigated for controlled drug release. Cells maintain an external pH (pHe) of approximately 7.4 and an intracellular pH (pHi) of approximately 7.2 under typical healthy conditions. However, due to increased glycolysis and lactic acid production known as the Warburg effect, cancer cells frequently exhibit a reversed pH gradient to a slightly more alkaline pHi (~7.4) and a more acidic pHe, ranging from 6.5 to 7.0 (Du et al., 2015). This acidic tumor microenvironment supports cancer progression, metastasis, and resistance to therapy, making it ideal for pH-responsive drug delivery systems (Hao et al., 2018, Worsley et al., 2022).

To exploit this characteristic, several in vitro studies have utilized artificial acidic conditions often pH 4.8 to mimic the tumor's intracellular compartments such as endosomes and lysosomes, which are naturally acidic. For example, Dadsetan et al. (2013) developed a pH-responsive microgels system for doxorubicin delivery and found that the release rate increased under acidic conditions, which are characteristic of tumor tissues, highlighting the potential for controlled delivery in acidic environments (Dadsetan et al., 2013). Also Yang and colleagues (2021) designed doxorubicin-loaded nanoparticles coated with a pH-sensitive polymer which were found to release the drug rapidly at acidic pH conditions (Yang et al., 2021). These studies demonstrate that using pH 4.8 in vitro models is valuable for evaluating the efficacy of drug delivery systems designed to release therapeutics in the acidic milieu of cancerous tissues or intracellular organelles. Thus, understanding and leveraging pH differences between cancerous and normal tissues holds significant promise in enhancing drug specificity and therapeutic outcomes.

Another approach is based on the use of external stimuli, such as light, magnetic fields, or ultrasound, to trigger drug release from functionalized nanoparticles. For example, magnetic nanoparticles have been used to deliver doxorubicin to cancer cells and release the drug under a magnetic field (Liu et al., 2019). External stimuli can provide precise control over drug release and spatial targeting. However, the delivery of external stimuli may require invasive procedures, and the safety and efficacy of some approaches are still under investigation (Pham et al., 2020)

A third approach involves the use of biological triggers, such as enzymes or specific cell surface receptors, to trigger drug release from functionalized nanoparticles. For example, nanoparticles coated with an enzyme-responsive polymer were found to release the drug in response to the presence of the enzyme matrix metalloproteinase-2 (MMP-2) in the tumour microenvironment (Naz et al., 2019). Biological triggers can provide selective drug release and reduce off-target effects. However, the specificity and selectivity of the trigger may be limited, and the efficacy of the approach may vary depending on the tumour type and stage.

In addition to these approaches, several strategies have been developed to optimize drug release kinetics, such as tuning the size, shape, and surface charge of the nanoparticles, as well as modifying the drug loading and release mechanisms (Mitchell et al., 2021). For example, lipid-coated nanoparticles have been shown to provide sustained release of paclitaxel over 7 days, with minimal burst release (Bai et al., 2022). Such strategies can improve the efficacy and safety of drug delivery but may require complex nanoparticle synthesis and characterization processes.

Overall, the selection of a drug release approach for functionalized nanoparticles should be based on the specific drug, the tumour microenvironment, and the desired release profile. Recent advancements in nanoparticle synthesis and characterization have enabled the development of more sophisticated drug delivery systems with improved drug release kinetics and therapeutic efficacy (Xia et al., 2021).

Researchers have reported that controlled drug release from functionalized nanoparticles is a key factor in the development of effective drug delivery systems for cancer treatment (Yao et al., 2020, Dang and Guan, 2020). Various approaches have been developed to achieve controlled drug release, each with its advantages and limitations. Further research is needed to

optimize these approaches and develop more personalized and effective drug delivery systems for cancer therapy.

3.12 Toxicity of iron oxide nanoparticles

Nanoparticle toxicity is a major concern in their application for cancer treatment. Several factors such as size, shape, surface chemistry, and composition affect nanoparticle toxicity. Several studies have evaluated the safety of Fe_3O_4NPs as drug-delivery vehicles. In one study, PEG-coated Fe_3O_4NPs were found to have low toxicity in mice for the assessed concentration (0.2 mg Fe mL^{-1}) and no significant histological changes were observed in the liver, spleen, and kidney (Lazaro-Carrillo et al., 2020). In another study, Fe_3O_4NPs functionalized with chitosan were found to have low toxicity and were able to effectively deliver siRNA to cancer cells (Zhou et al., 2017). Furthermore, Fe_3O_4NPs have been used in clinical trials for drug delivery applications with promising results.

The safety of Fe_3O_4NPs is influenced by various factors, including their size, surface charge, and functionalization. Small Fe_3O_4NPs have been shown to have higher toxicity compared to larger ones (Zhang et al., 2022). Furthermore, surface functionalization can impact the toxicity of Fe_3O_4NPs. For example, PEGylation of Fe_3O_4NPs has been shown to improve their biocompatibility and reduce toxicity. Song reported that modified superparamagnetic Fe_3O_4NPs were tested in vitro and showed no significant cytotoxicity. In vivo imaging studies also showed that the modified Fe_3O_4NPs had improved contrast properties and were able to target specific tissues. These findings suggest that biomimetic modification of Fe_3O_4NPs could enhance their safety and effectiveness for use in biomedical applications (Song et al., 2019). Liu also reported the low toxicity of PEG-coated AuNPs in cancer cells. In addition, the route of administration and the dose of Fe_3O_4NPs can also impact their safety.

In conclusion, Fe_3O_4NPs have shown great potential as drug delivery vehicles, but their safety must be carefully evaluated. The toxicity of Fe_3O_4NPs is influenced by various factors, including their size, surface charge, and functionalization. Further studies are needed to fully understand the safety of Fe_3O_4NPs and to develop safe and effective drug delivery systems.

3.13 Drug Release Kinetics

Drug release kinetics is a critical aspect of nanoparticle-based drug delivery systems. The release kinetics of drugs from nanoparticles can be controlled by various factors such as

nanoparticle size, surface chemistry, and drug properties. Several mathematical models have been developed to describe the release kinetics from functionalized nanoparticles. For instance, the Higuchi model has been widely used to describe the drug release kinetics from nanoparticles (Cong et al., 2018). These models are based on different kinetic assumptions and are used to fit experimental data and predict drug release profiles. Some of the common drug release kinetics models include zero-order kinetics, first-order kinetics, second-order kinetics, the Higuchi model, the Korsmeyer-Peppas model, and the Weibull model (Dash et al., 2010). The selection of a particular model depends on the mechanism of drug release and the physicochemical properties of the NPs. These models are widely used in the design and optimisation of drug delivery systems for cancer treatment (Li et al., 2019).

Although significant progress has been made in the development of functionalized nanoparticles for the controlled release of drugs in cancer treatment, several gaps remain in the literature. Firstly, there is a need to optimise the drug loading and release efficiency of functionalized nanoparticles. Secondly, the long-term toxicity and biocompatibility of functionalized nanoparticles need to be evaluated. Thirdly, more studies are required to investigate the drug release kinetics from functionalized nanoparticles in vitro and vivo, also improving stability. Finally, the development of targeted functionalized nanoparticles for specific cancer types is an area that requires further exploration.

3.13.1 Zero-order kinetics

Zero-order drug release kinetics refers to a type of drug release pattern where the rate at which a drug is released from a pharmaceutical dosage form, such as a tablet or capsule, remains constant over time (Paarakh et al., 2018). This means that a consistent amount of the drug is released per unit of time, regardless of the concentration of the drug in the dosage form or the surrounding environment (Laracuente et al., 2020).

The linearized equation for zero-order drug release kinetics is:

$$Q_t = -K_0 \cdot t + Q_0 \qquad [1]$$

Where:

Q_t the amount of drug released at time t

K_t is the zero-order release rate constant.

t is the time.

Q_0 is the initial amount of drug in the dosage form (at t=0).

Zero-order drug release kinetics are desirable in certain pharmaceutical applications because they provide a controlled and steady release of the drug (Gokhale, 2014). This can be particularly important for drugs that have a narrow therapeutic window, where maintaining a constant drug level in the body is crucial for safety and efficacy.

3.13.2 First-order drug release kinetics

First-order drug release kinetics, in the context of pharmaceuticals, refers to a type of drug release pattern where the rate of drug release is directly proportional to the remaining amount of the drug in a pharmaceutical dosage form (Singhvi and Singh, 2011). That is, the rate of drug release increases as the concentration of the drug in the dosage form decreases. This leads to an exponential decrease in the drug release rate over time.

The model predicts that a certain fraction or percentage of the drug remaining in the dosage form is released per unit of time. Mathematically, this relationship can be described using the first-order kinetic equation (Paarakh et al., 2018).

$$Q_t = Q_0 . e^{-k \cdot t} \qquad [2]$$

Where:

Q_t is the amount of drug released at time t.

Q_0 is the initial amount of drug in the dosage form (at t=0).

k is the first-order release rate constant.

t is the time.

e is the base of the natural logarithm.

The linearized equation for zero-order drug release kinetics is:

$$\ln Q_t = -K_0 \cdot t + \ln Q_0 \qquad [3]$$

First-order drug release kinetics is utilized to provide controlled and sustained drug release over time (Donbrow and Friedman, 1975). However, the drug release rate decreases as the drug concentration in the dosage form decreases, which can lead to fluctuations in drug levels in the body (Herdiana et al., 2022). Therefore, different drug delivery systems and formulations may

be employed to modify these release kinetics according to the specific therapeutic goals of medication.

3.13.3 Second-order drug release kinetics

Second-order drug release kinetics, also known as second-order release, is a type of drug release pattern in pharmaceutical science and drug delivery systems (Gupta and Purwar, 2021). In this context, second-order kinetics refers to a release mechanism where the drug release rate is directly proportional to the square root of the remaining amount of drug in a pharmaceutical dosage form.

Mathematically, second-order drug release kinetics can be described using the following equation:

$$Q_t = Q_0 - k \cdot t^2 \qquad [4]$$

Where:

Q_t is the amount of drug released at time *t.*

Q_0 is the initial amount of drug in the dosage form (at t=0).

k is the second-order release rate constant.

t is the time.

The linearized equation for second-order drug release kinetics is:

$$\frac{1}{Qt} = kt + \frac{1}{Q0} \qquad [5]$$

In this type of release mechanism, the drug release rate increases as the remaining drug concentration decreases, but it does so in a quadratic or nonlinear manner due to the t^2 term in the equation. This can lead to a more sustained release compared to first-order kinetics, which results in exponential drug release over time (Paarakh et al., 2018).

Second-order drug release kinetics are employed in specific drug delivery systems and formulations to achieve different drug release profiles based on therapeutic needs (Singhvi and Singh, 2011). It can provide a prolonged and controlled release of a drug, which may be suitable for certain medications and clinical applications.

3.13.4 Higuchi Drug Release Kinetics

Higuchi drug release kinetics, also known as Higuchi's equation, is a mathematical model used to describe the release of a drug from a pharmaceutical dosage form (Paarakh et al., 2018). This model is named after the Japanese pharmacologist Takeru Higuchi, who proposed it in the 1960s. Higuchi's equation describes the release of a drug from a solid, non-erodible matrix, such as a tablet, and is based on Fick's law of diffusion (Kalam et al., 2007). It is used to explain the relationship between the cumulative amount of drug released (Q_t) and the square root of time(t):

$$Q_t = K \cdot \sqrt{t} \qquad [6]$$

Where:

Q_t is the cumulative amount of drug released at time t.

K is a constant specific to the drug and the dosage form.

Higuchi drug release kinetics suggest that drug release from such solid dosage forms is primarily driven by a diffusion process, where the drug molecules move through the matrix and are released into the surrounding medium (Shoaib et al., 2006). The square root of time indicates that, as time progresses, the rate of drug release decreases, resulting in a more sustained release profile.

Higuchi's equation is commonly used to analyze and design controlled-release drug delivery systems where a gradual and consistent release of a drug is desired (Paarakh et al., 2018). It provides a fundamental understanding of the drug release process and helps in optimizing the formulation of pharmaceutical products for controlled drug delivery.

3.13.5 Korsmeyer-Peppas drug release Kinetics model

The Korsmeyer-Peppas model, also known as the Korsmeyer-Peppas drug release kinetics or the Power Law model, is a mathematical model frequently used to describe drug release from pharmaceutical dosage forms, particularly in the context of controlled-release drug delivery systems (Permanadewi et al., 2019). This model is an extension of the Higuchi model and is often used to analyze non-Fickian or anomalous drug release, where release behaviour deviates from simple diffusion.

The Korsmeyer-Peppas equation is represented as follows:

$$\frac{Mt}{M\infty} = K.t^n \quad [7]$$

Where

M_t is the amount of drug released at time t.

M_∞ is the total or maximum amount of drug that can be released.

K is a constant related to the characteristics of the drug and the pharmaceutical formulation.

t is the time.

n is the release exponent, which provides information about the mechanism of drug release:

If $n = 0.5$, it indicates Fickian diffusion (Higuchi model).

If $0.5 < n < 1.0$, it suggests anomalous or non-Fickian release, involving a combination of diffusion and other mechanisms.

If $n=1.0$, it indicates Case II transport, where the drug release is dominated by polymer relaxation.

If $n > 1.0$, it suggests super case II transport.

The Korsmeyer-Peppas model allows researchers to determine the release exponent (n) and, thereby, gain insight into the underlying mechanisms controlling drug release from a particular dosage form (Paarakh et al., 2018). This model is particularly useful when dealing with complex release patterns, such as those observed in polymeric matrices and other controlled-release systems. It is commonly employed in pharmaceutical and biomaterial sciences to study and design drug delivery systems for various therapeutic applications (Rehman et al., 2020).

3.14. Recent Advancement in Nanoparticle based drug Delivery systems

Nanoparticle-based drug delivery systems have emerged as a transformational platform in oncology, providing more selectivity, lower systemic toxicity, and better therapeutic outcomes. Traditional chemotherapy is frequently hampered by low absorption, nonspecific distribution, and significant adverse effects. Recent advances in nanotechnology are tackling these

constraints by allowing for site-specific delivery of anticancer drugs, better pharmacokinetics, and real-time monitoring of therapy outcomes.

A significant advancement in this field is the development of ligand-functionalized nanoparticles that are designed to target specific biomarkers expressed on cancer cells. Overexpressed receptors include the folate receptor alpha, the epidermal growth factor receptor (EGFR), and the human epidermal growth factor receptor 2 (HER2). These approaches improve drug accumulation at the tumor site and reduce off-target toxicity by functionalizing nanoparticles with ligands such as antibodies, peptides, or aptamers, resulting in selective absorption by tumor cells via receptor-mediated endocytosis (Zhou et al., 2022).

These carriers frequently include imaging agents (such as MRI or fluorescence contrast materials) in addition to chemotherapeutic medicines, allowing for concurrent therapy and tumor response monitoring. Gold nanoparticles, for example, are often utilized due to their optical characteristics and biocompatibility; when coupled with photothermal agents and anticancer medications, they enable for dual photothermal-chemotherapy, resulting in synergistic anticancer effects (Wang et al., 2023).

Collectively, these recent advancements in nanoparticle-based drug delivery systems represent a major leap forward in the precision and personalization of cancer therapy. As these technologies progress through preclinical and clinical stages, they hold the potential to significantly improve therapeutic efficacy while minimizing adverse effects, marking a paradigm shift in oncological treatment.

We have established that different methods are used for Synthesis, Characterization, and Drug Loading. Furthermore, Controlled Drug Release can be achieved by encapsulating the drug in a polymer like PEG, also drug release can be triggered by various factors like pH. Lastly, the literature provides that Drug Release Kinetics can be established using mathematical models such as Higuchi, and the Korsmeyer-Peppas model.

Preclinical studies have demonstrated the efficacy of functionalized Fe_3O_4NPs for Docetaxel delivery in various cancer models, showcasing improved therapeutic outcomes and reduced systemic toxicity compared to free Docetaxel. Encouraged by these findings, we synthesized functionalized Pegylated Fe_3O_4NPs for Controlled released Docetaxel vitro a step forward in increasing the stability of the Docetaxel loaded Fe_3O_4NPs. We also studied the Docetaxel release kinetics at different pH levels to appreciate the stability of the delivery system at

physiological pH which is a step in the right direction that has the potential to reduce Docetaxel accumulation in normal cells.

Chapter Four

Experimental Techniques and Characterization

4.1 Materials

Iron trichloride hexahydrate ($FeCl_3 \cdot 6H_2O$) reagent grade, ≥98%, Iron dichloride tetrahydrate ($FeCl_2 \cdot 4H_2O$) reagent grade, ≥99 %, Folic acid ≥97% Bioreagent ammonium hydroxide reagent grade, 98%, Polyethylene Glycol(PEG-8000) BioUltra, 8000≥99.0% (GC), 28% Ammonium Hydroxide (NH_4OH)≥98%, *N*-(3-dimethylamino propyl)-*N*-ethyl carbodiimide (EDC)≥99.0%, Tetrahydrofuran(THF) ≥99.0%, N-Hydroxysuccinimide(NHS) ≥99.0%, 2-Morpholinoethanesulfonic acid, Dichloromethane(DCM) ≥98%, 4-(dimethylamino) pyridine (DMAP) ≥98%, were all purchased from Merck. Docetaxel was donated by the University Teaching Hospital (UTH), University of Zambia (UNZA). Acetone ≥99.5%, ethanol ≥ 99.5%, and chloroform ≥99.0% were purchased from Sigma-Aldrich. All chemicals and solvents in this work were used as received.

4.2 Instrumentation

Fourier transform infrared (FT-IR), a Perkin Elmer Spectrum RXI FT-IR spectrometer, Shimadzu 2000 UV-Vis spectrophotometer, and X-ray Diffraction (XRD) Olympus TERRA-538, were used for characterization.

4.3 Preparation of materials

4.3.1 Synthesis of Iron oxide Nanoparticles (Fe_3O_4NPs).

Synthesis of Fe_3O_4 magnetic nanoparticles was done by co-precipitation of iron trichloride hexahydrate ($FeCl_3 \cdot 6H_2O$) and iron dichloride tetrahydrate ($FeCl_2 \cdot 4H_2O$) using the earlier reported method (Singogo, 2022). Briefly, 15.20 g of $FeCl_3 \cdot 6H_2O$ and 5.30 g of $FeCl_2 \cdot 4H_2O$ were dissolved into 200 mL of deionized water. The mixture was then stirred for 30 minutes, and chemical precipitation was achieved by adding 2.0 M NaOH solution. The reaction system ran for 1.5 hr. Co-precipitation of Fe_3O_4 NPs was completed at pH 9. The precipitates were separated by a permanent magnet and washed with deionized water until pH neutral. Finally, Fe_3O_4 NPs were washed with acetone and dried in an oven at 70 ^{o} C.

4.3.2 Synthesis of the Iron Oxide Folate Conjugate (Fe_3O_4@FA)

Magnetic iron oxide NPs were functionalized with folic acid (FA) using a method reported by (Ancira-Cortez et al., 2017a) with a few modifications. Briefly, a solution of FA (0.055 g) in 5mL of dichloromethane (DCM). The solution was mixed with an ethanolic solution of *N*-(3-dimethylaminopropyl)-*N*-ethylcarbodiimide (EDC) (0.582 g in 50 mL) and 4-(dimethylamino) pyridine (DMAP) (0.045 g in 50 mL). The solution was then sonicated using a high-intensity ultrasound probe for 2 hr and then allowed to stand overnight. Furthermore, the solution was shaken vigorously at room temperature for 24 hr, and the Fe_3O_4NPs@FA was recovered and washed *via* magnetic decantation, using deionized water. The product was stored for use in the subsequent steps.

4.3.3 Docetaxel loading onto Iron Oxide Folate Conjugate (Fe_3O_4@FA)

Drug loading was conducted using a covalent method, briefly 20 mg of Fe_3O_4@FA was ultrasonically dispersed in a 20 mL solution of Docetaxel (DXL) in water (DXL conc 1mg mL^{-1}) for 15 min. The suspension was left under shaking for 24 hr at room temperature and protected from light using aluminium foil. Fe_3O_4@FA@DXL was collected using magnetic decantation and washed with distilled water until the supernatant became clear, indicating the absence of free DXL particles in the wash (Thambiraj et al., 2021, Day et al., 2021).

4.3.4 Encapsulation of Fe_3O_4@FA@DXL using Poly (Ethylene) Glycol (Fe_3O_4@FA@DXL@PEG).

PEGylation of Fe_3O_4@FA@DXL was carried out using a method used by (Thambiraj et al., 2021) with modification. Briefly, 2.0 mg of PEG 8000 was dissolved in 5.0 mL of distilled water, then added drop-wise into 100 mL of 1.0 mM concentration of Fe_3O_4@FA@DXL solution and shaken for 12 hr at room temperature. After encapsulation, the solution was maintained at the pH range of 6.5 to prolong the stability of the Fe_3O_4@FA@DXL@PEG nanoparticles. Further, the Fe_3O_4@FA@DXL@PEG were collected using magnetic decantation, stored, and characterized.

Experimental Design

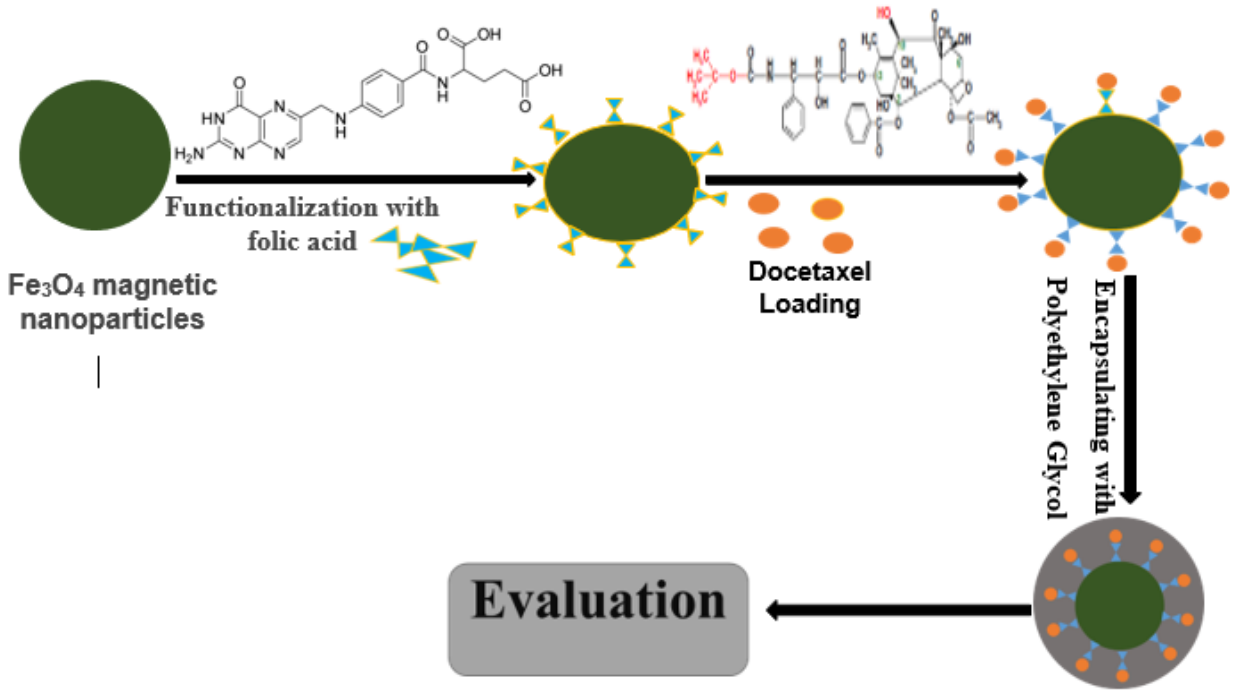

Figure 2: Experimental Design for the Synthesis of Docetaxel-loaded Iron Oxide Nanoparticles

4.4 Nomenclature of multilayered nanoparticles

The design above is of a multilayered polymer nanoparticle (MLNP), comprising of Iron Oxide nanoparticles named as Fe_3O_4NPs. The surface was functionalized with Folic acid (FA), hereby referred to as Fe_3O_4@FA. Then loaded with Docetaxel (DXL) named Fe_3O_4@FA@DXL and finally encapsulated with Polyethylene Glycol(PEG). The full name of the MLNP is Fe_3O_4@FA@DXL@PEG. The symbol @ represents the addition of a layer on the core nanoparticle.

4.5 Characterization

The Structural analysis included UV-VIS measurements recorded using a Shimadzu 2000 UV-Vis spectrophotometer. The absorbance measurements were taken for Fe_3O_4 NPs, Fe_3O_4@FA, Fe_3O_4@FA@DXL, Fe_3O_4@FA@DXL@PEG, and pure samples of each FA, DXL, and PEG 8000 using a 1.0 mL cuvettes from which different spectra were obtained. The crystal structure of the products was characterized by X-ray Diffraction (XRD) Olympus TERRA-538. The patterns with the Co Kα radiation (λ = 1.7889 Å) at 30.3 kV, 0.006 mA were recorded in the

region of 2θ range 0 to 55° for both the Fe_3O_4 nanoparticles and Fe_3O_4@FA. Briefly, Fe_3O_4 NPs and Fe_3O_4@FA were crushed and sieved using a 100-micrometer sieve. Then about 5mg of each sample was loaded on a slide, the XRD machine. The FT-IR spectra were recorded using KBr powder on a Perkin Elmer Spectrum RXI FT-IR spectrometer. The samples were scanned over a range of 400 cm^{-1} to 4000 cm^{-1}.

4.6 Drug Release Studies

Drug release experiments were carried out on both Pegylated and unPegylated Docetaxel-loaded Iron Oxide nanoparticles. Briefly, 50 mg of the unPegylated nanoformulation was suspended in 20 mL Phosphate Buffer saline (PBS) at pH 4.80, and absorbance was taken at intervals for 72 hr. Then Pegylated nanoparticles were also suspended in PBS at pH 4.80, 6.00, 7.00 and 7.45, taking the absorbance for 72 hr. For each sample, the experiment was repeated thrice, and the mean was calculated.

Chapter Five

Results And Discussion

5.1 Introduction

This chapter focuses on the presentation of results obtained from experimental work and discusses each of the findings. These include structural analysis results obtained using FT-IR and UV-Vis spectrometers and those for morphology characterization from XRD. The results from the adsorption, and drug release experimental results are also discussed.

5.2 Ultraviolet-Visible spectroscopy analysis

The UV-Vis studies were carried out to validate the formation of Iron oxide nano particles and subsequent modifications as shown in Figure 3. The synthesized Fe3O4NPs showed a continuous absorption in the visible range of 200- 700 nm. It can be observed that the spectra that the absorption peaks shifted slightly towards the higher wavelength after addition of FA. The shift was attributed to an increase in the particle size and it is in perfect agreement with (Singogo, 2022).

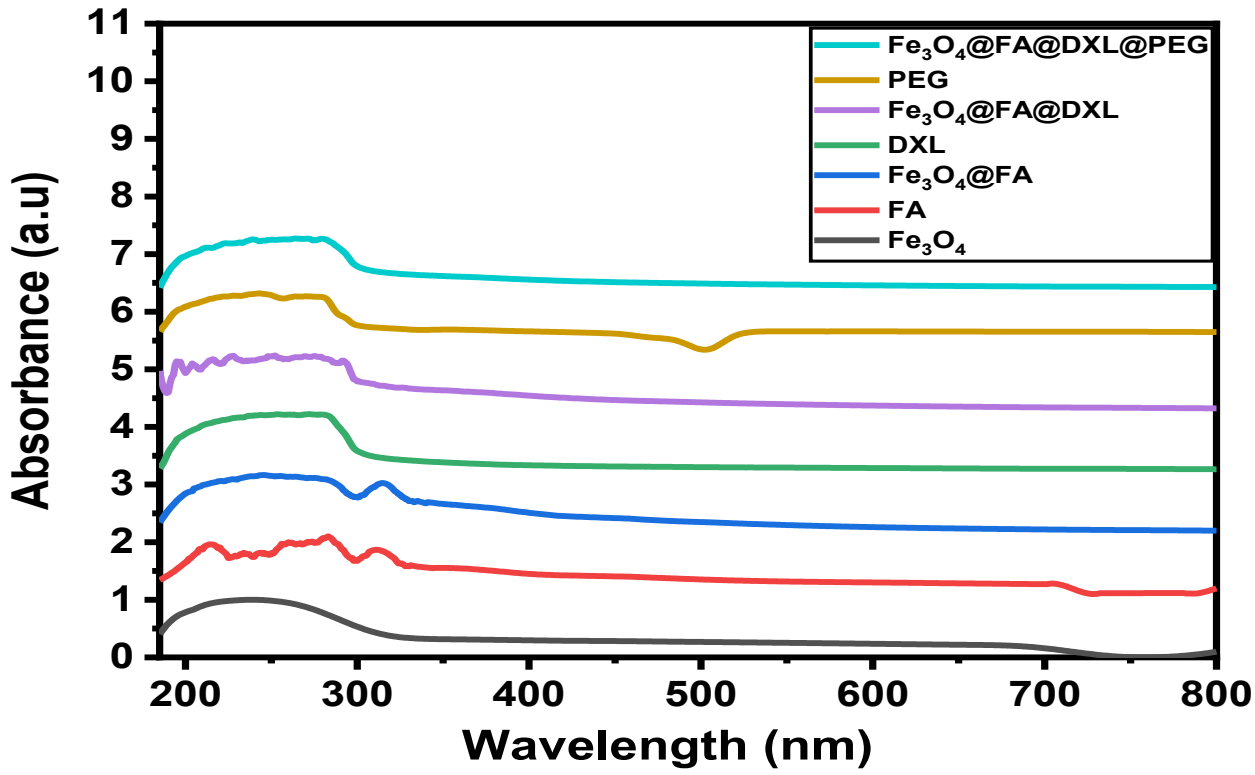

Figure 3: UV-Vis spectra of Fe_3O_4 NPs, FA, Fe_3O_4@FA, DXL, Fe_3O_4@FA@DXL, PEG and Fe_3O_4@FA@DXL@PEG

The folic acid peak was observed at 285 nm and 320 nm (Pourjavadi et al., 2016, Wei et al., 2017), this peak shows that there were structural changes on the surface of Fe_3O_4NPs due to folic acid functionalization. UV–Vis spectra of the DXL were observed at 231 nm ascribed to π–π* transition of carbonyl and hydroxyl groups were present in the sample (Rivero-Buceta et al., 2019). Also, observable is the peak at 528 nm characteristic of PEG which disappeared after PEGylating the DXL-loaded Fe_3O_4NPs These results indicate the formation of Fe_3O_4NPs drug delivery system with step-by-step conjugation of FA, DXL, and PEG. Figure 4 shows the step-by-step development of the Pegylated docetaxel-loaded systems, the spectra of the intermediates and pure compounds used for modifications are shown. It is observed that pure folic acid (FA) showed a notable peak at about 320 nm, the same peak is observed on the functionalized iron oxide nano particles (Fe_3O_4@FA). The same trend was observed with pure DXL and PEG, this was observed also by Singogo (Singogo, 2022) and Wei et al (Wei et al., 2017).

5.3 X-Ray Diffraction Spectroscopy Analysis

The XRD data of iron oxide magnetic nanoparticles agree with the standard value of Fe_3O_4 (JCPDS file no: 19-0629). XRD analysis of the particles (Figure 4) shows well-defined Bragg reflection characteristics of Fe_3O_4. The data shows diffraction peaks at $2\Theta = 21.3°, 31.0°, 35.1°$, 41.38°, 45.86°, and 50.52°, which can be indexed to the (111), (200), (220), (311), (222), and (400) planes of Fe_3O_4 in a cubic phase, respectively, which are characteristics of Fe_3O_4 nanoparticle diffraction pattern according to JCPDS standard data 19-0629. These results are in perfect agreement with (Mishra and Sardar, 2015)**.** The height of the peaks is reduced from Fe_3O_4 NPs to Fe_3O_4@FA as the particle increases. The reduction in peak height and disappearance of some peaks on the Fe_3O_4@FA pattern can be attributed to the effect of the FA masking of the Fe_3O_4 nanoparticle. It can be seen from an XRD diffraction pattern that synthesized iron oxide nanoparticles have high purity and good crystal quality. Moreover, the broadening of the diffraction peaks confirms the small particle size and high crystalline nature of the material which agrees with (Ali et al., 2013, Singogo, 2022).

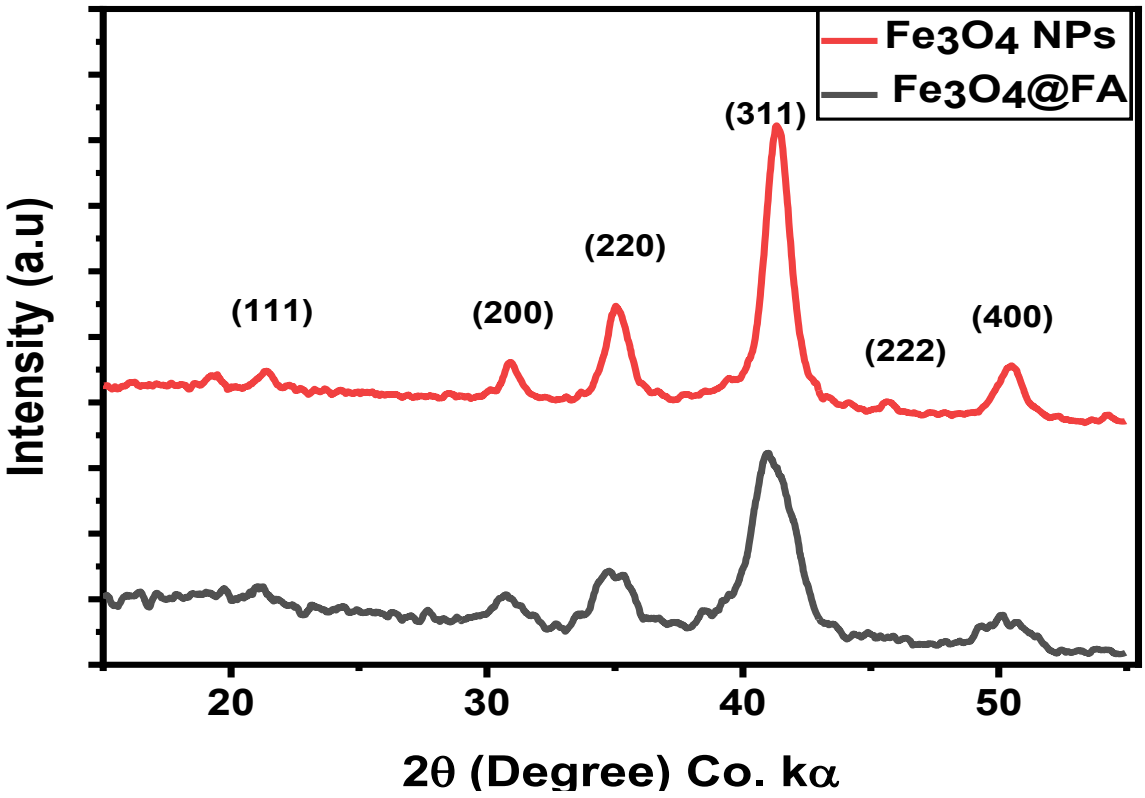

Figure 4: XRD patterns for Fe_3O_4 NPs, and Fe_3O_4@FA

The average crystallite size of nanoparticles was estimated using the Debye Scherrer formula

$$D = \frac{k\lambda}{\beta cos\theta}$$

Where D is the crystallite mean size, k is a shape function for which a value of 0.94 for spherical crystalline, λ is the wavelength of the radiation in nm, β is the full width at half-maximum (FWHM) in the 2θ scale in radians and θ is the Bragg angle. It was found that the average crystallite size of magnetic nanoparticles was 10.53 nm.

5.3 Fourier Transform Infrared Spectral Analysis

The spectrum of magnetic Fe_3O_4 nanoparticles is depicted in Figure 5(a), the characteristic absorption of the Fe-O bond appears at 558 cm^{-1} and it is in perfect agreement with (Ebadi et al., 2023, Singogo, 2022). The peaks at 1637, 2038, and 3406 cm^{-1} also are in agreement with the spectra observed by Wei and his colleagues (Wei et al., 2012). This further indicates that

iron (Fe) is the key structural element in the compound (Stoia et al., 2016). After functionalizing with Folic acid, new peaks were observed, the prominent ones being 1689 cm^{-1} (figure 5b), which is characteristic of the C=O vibrations, which is in agreement with (Jalilian et al., 2011), 1259, 1549, and 2340 cm^{-1} attributed to the C=C vibrations of the aromatic ring and a broad band from 2971 to 3409 cm^{-1} characteristic of O-H stretching of folic acid. These were also observed by Selvarathinam (Selvarathinam and Dhesingh, 2022, Ancira-Cortez et al., 2017b). Figure 5c shows the spectrum after loading the Fe_3O_4@FA with DXL, significant peaks included the ones 1580, 1720, 2342, and 3410 cm^{-1}(Rivero-Buceta et al., 2019) the broad peak for carboxylic acid OH diminished, confirming a change in the functional group from carboxylic acid to an ester, the results are in perfect agreement with already published work (Selvarathinam and Dhesingh, 2022). The slight shift of the peak from 1689 to 1720 could be a result of the ester C=O instead of carboxylic acid C=O. The major peaks of DXL disappeared in the FT-IR spectra after encapsulating with PEG 8000 (Figure 5d), indicating that DXL was fully encapsulated in PEG (Baek and Cho, 2015). The observed peak around 1324 is a result of C-O-C stretching in PEG 8000.

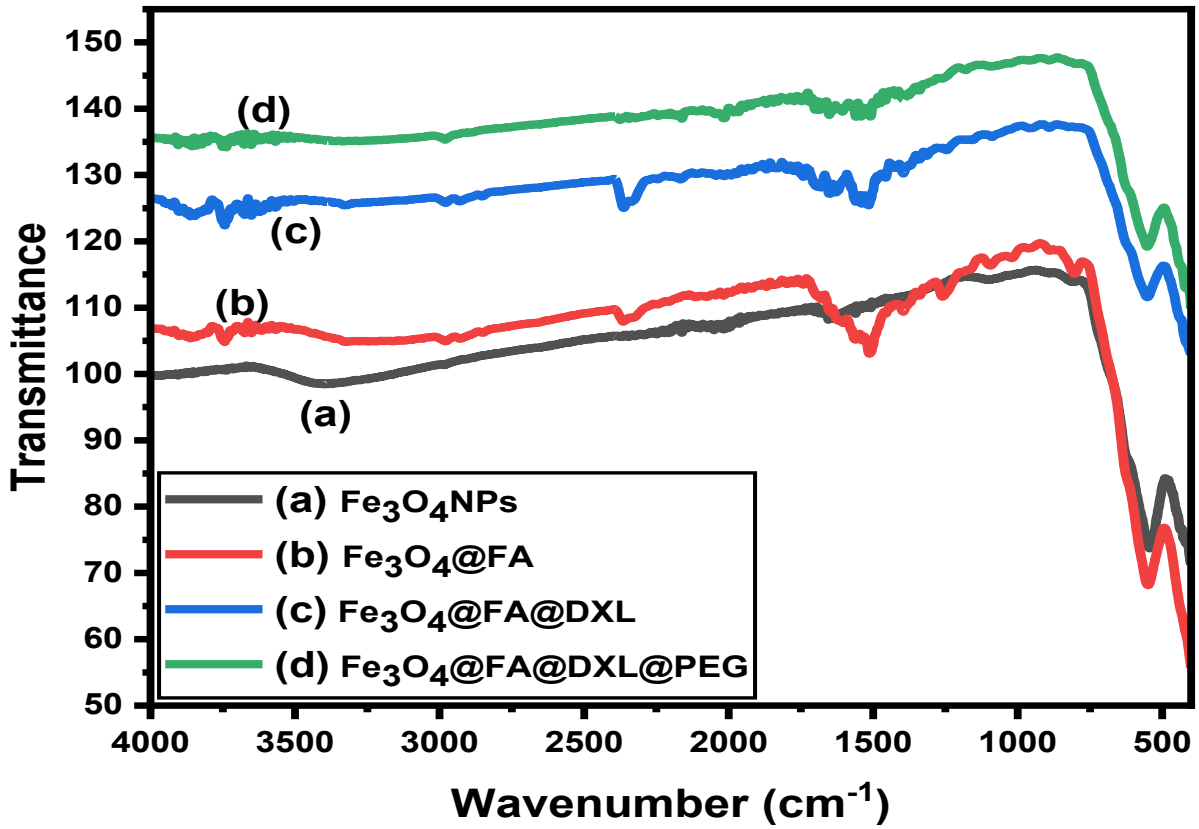

Figure 5: FT-IR Spectra of (a) Fe_3O_4 NPs (b) Fe_3O_4@FA (c) Fe_3O_4@FA@DXL and (d) Fe_3O_4@FA@DXL@PEG.

The spectra above show the changes in peak strength due to changes in functional groups added to the Iron Oxide nanoparticles. Some peaks disappeared while others appeared as different molecules were added to the metallic core.

5.5 Adsorption Isotherms

Adsorption isotherms play a crucial role in understanding drug loading onto various carriers. They are useful in understanding drug adsorption and release of the drug delivery system (McCarthy et al., 2017). They provide insights into the maximum capacity of a carrier to adsorb the drug. This helps in optimizing the formulation to achieve the desired drug loading while avoiding wastage of materials. Also, optimization of Formulation, this helps to understand the conditions under which maximum drug loading can be achieved. This optimization is essential for formulating efficient drug delivery systems, ensuring the effective delivery of therapeutic agents to target sites (Schmid et al., 2023).

Different carriers exhibit different adsorption behaviors, which can be elucidated through adsorption isotherms experiments (Nyirenda et al., 2022). Understanding these behaviors helps in selecting suitable carriers for drug delivery systems based on factors like surface area, pore size, and affinity for the drug molecule. Adsorption isotherms also provide insights into the release kinetics of drugs from carriers. By understanding the adsorption-desorption dynamics, a design of formulations with controlled release properties can be achieved, allowing for sustained drug release over an extended period, which is vital for achieving therapeutic efficacy and minimizing side effects (Selvarathinam and Dhesingh, 2022).

These set of experiments are significant for drug loading as they provided critical information for optimizing formulation, selecting suitable carriers, controlling drug release kinetics, and ensuring the stability of the formulation over time (Papachristos et al., 2023). This understanding contributed to the development of efficient and effective drug delivery system.

Some of the parameters determined are;

Adsorption efficiency (%) and adsorption capacity at equilibrium (Q_e), were determined using equations (8) and (9);

$$Adsorption\ efficiency\ (\%) = \frac{(Co - Ce) \times 100}{Co} \quad [8]$$

$$Adsorption\ capacity\ (qe)\ = \frac{(Co - Ce) \times V}{m} \quad [9]$$

Where C_o (mg/L) is the concentration of folic acid before adsorption, C_e (mg/L) is the equilibrium concentration of folic acid Q_e (mg/g) is the amount of folic acid adsorbed at equilibrium, m (g) is the mass of the Fe_3O_4NPs used, and V (L) is the volume of folic acid solution used.

Table 1. Concentration of Folic acid and amount bound in the sample solutions

Initial Concentration	Equilibrium Concentration	Bound FA
mg/L	mg/L SD [n=3]	mg/L
1.00	0.90 ± 0.002	0.10
2.00	1.90 ± 0.002	0.10
4.00	3.84 ± 0.002	0.16
6.00	5.80 ± 0.001	0.23
8.00	7.72 ± 0.001	0.28
10.00	9.68 ± 0.002	0.32
12.50	11.82 ± 0.001	0.68
14.50	13.52 ± 0.002	0.88
16.50	15.68 ± 0.001	0.82

Table 1 shows that there was a decrease in the concentration of folic acid in the solution due to binding on the Fe_3O_4 NPs. In the studied concentration range, the folic acid adsorption amount increases with the increasing amount of the folic acid initial concentration. This is consistent with already published work by (Hamedani and Felrgari, 2017, Castillo et al., 2015). At the 16.50 mg/L, the bound folic acid decrease compared to the one at 14.50 mg/L suggesting that about 15.00 to16.00 mg/L of folic acid is needed for maximum functionalization of the Iron oxide nanoparticles.

5.5.1 Adsorption isotherms models

The Langmuir Freundlich and Temkin isotherms are common mathematical models used to describe the adsorption of molecules onto a surface.

Langmuir adsorption isotherm: The Langmuir isotherm is a model that assumes that the adsorption of molecules onto a surface occurs through a monolayer process. The sites of adsorption have equal affinity for adsorption and the interaction of adsorbed molecules is restricted. In other words, once a molecule adsorbs onto the surface, it does not allow any other molecules to adsorb onto the same site. The isotherm for single solute adsorption can be represented as follows:

$$Q_e = \frac{1}{qmKL} + \frac{Ce}{qm} \quad [10]$$

The linear equation is written as:

$$\frac{Ce}{qe} = \frac{1}{qmKL} + \frac{Ce}{qm} \quad [11]$$

Where q_e (mg/g) is the amount of folic acid adsorbed at equilibrium, C_e (mg/L) is the equilibrium concentration of folic acid, Q_{max} (mg/g) is the maximum adsorption capacity and K_L (L/mg) is the Langmuir constant which measures the affinity of folic acid towards the adsorbent adsorption sites. Thus, the magnitude of K_L indicates either a strong or weak interaction between the folic acid and the adsorption sites of the adsorbent. The parameters q_m and K_L were determined from the plot of C_e/qe versus C_e. The separation factor, R_L, was determined from the equation below.

$$R_L = \frac{1}{1 + KLCi} \quad [12]$$

Where R_L is the separation factor, Ci (mg/L) is the highest initial concentration of folic acid and K_L is the Langmuir constant. The value of the separation factor indicates the favorability of the adsorption process.

The Freundlich isotherm model: shows an empirical relationship that describes the heterogeneity of sorbent surface and reflects as multilayer adsorption, expressed below:

$$Qe = KFCe^{1/n} \quad [13]$$

Taking the natural log gives the linear form of the Freundlich isotherm shown below.

$$lnQe = lnKF + \frac{1}{n} lnCe \qquad [14]$$

Q_e and C_e have the same meaning as in the Langmuir isotherm, while K_F and n refer to the Freundlich constants. K_F is linked to the adsorbent's binding energy, while n is the heterogeneity factor that quantifies the degree of non-linearity between adsorption and solution concentration. A value between 1 and 10 for n indicates favourable adsorption. When plotting $\ln Q_e$ versus $\ln C_e$, the result is a straight line with a slope of $\frac{1}{n}$ and an intercept of $\ln K_F$.

Figure 6 below shows the Langmuir isotherm linear plot, while Figure 7 shows Freundlich and Figure 8 the Temkin Adsorption Isotherm plot.

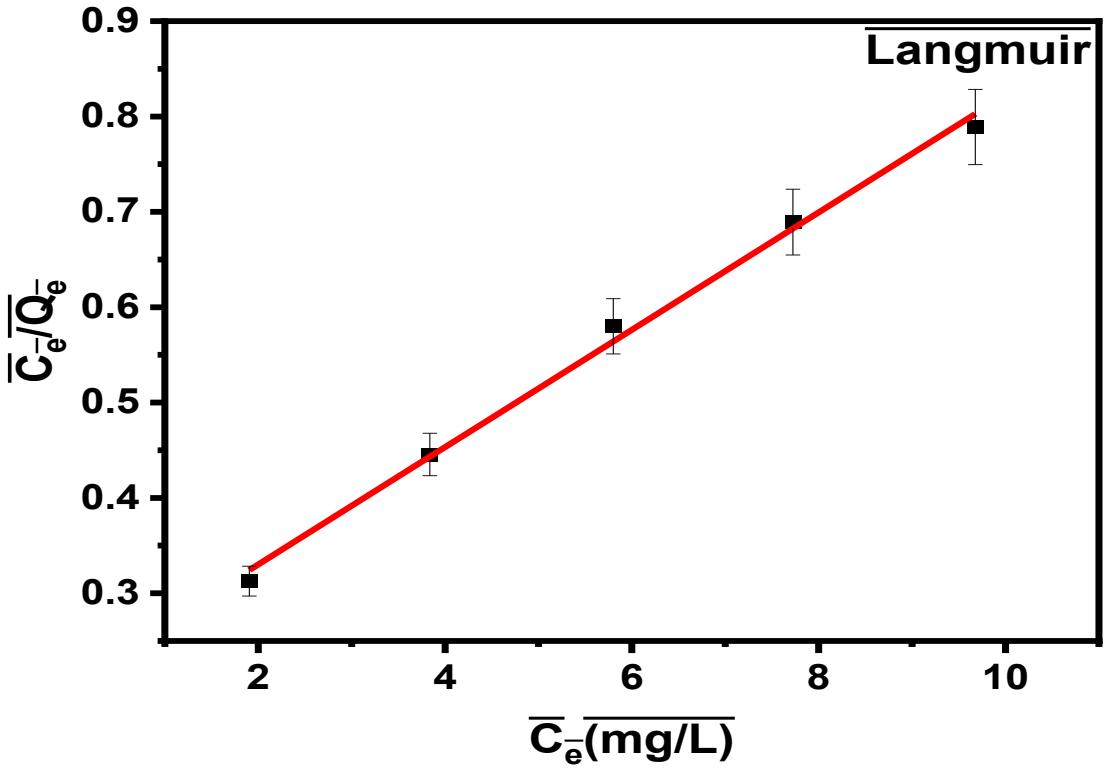

Figure 6: The Langmuir Isotherm model plot

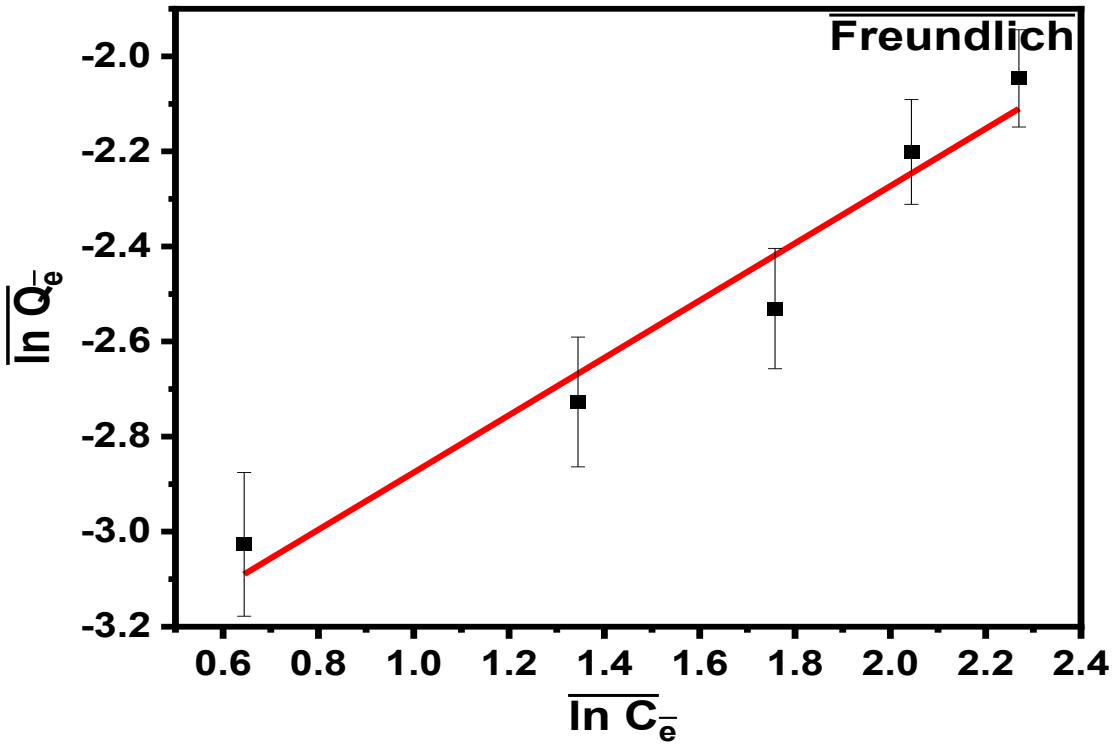

Figure 7: The Freundlich Adsorption Isotherm plot

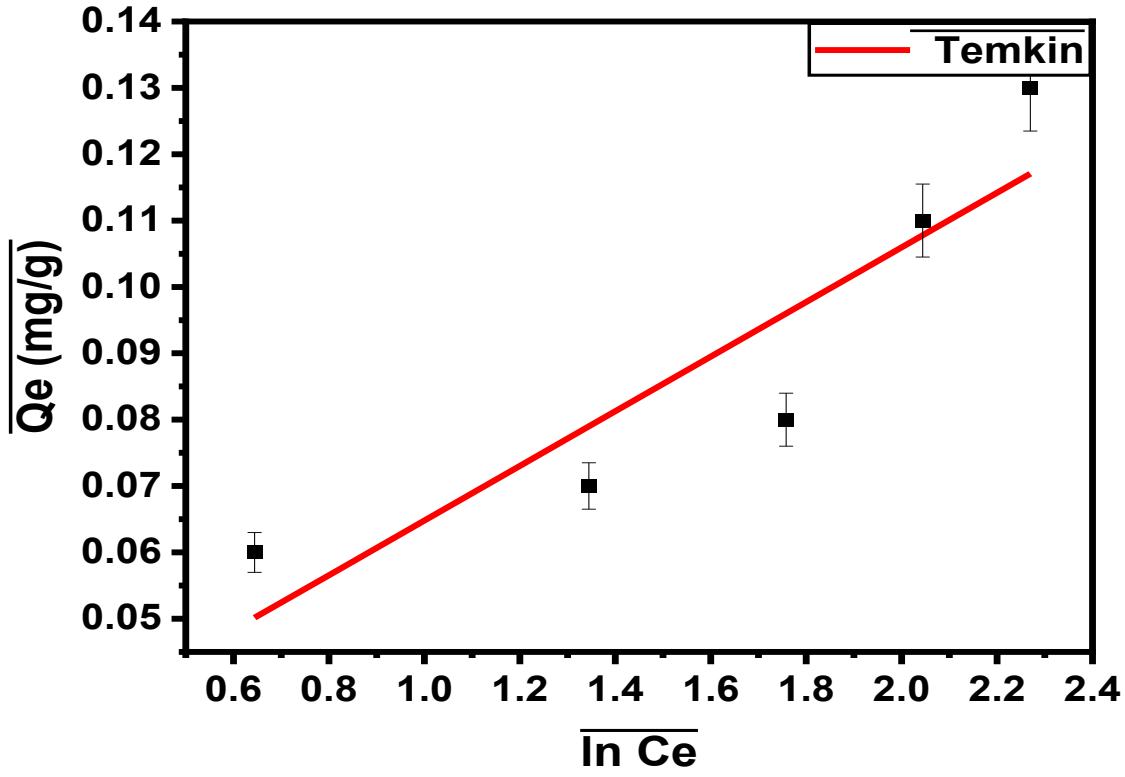

Figure 8: The Temkin Adsorption Isotherm plot

The three models examined above showed a perfect linear curve for the Langmuir (Figure 6) compared to the Freundlich (Figure 7) and Temkin (Figure 8). Table 2 below comprise of a summary of the respective parameters of the three isotherm models.

Table 2. Langmuir, Freundlich and Temkin model parameters

Type of Isotherm	Parameter	value
Langmuir	Q_{max}	16.239
	K_L	0.29746
	R_L	0.2516
	R^2	0.9947
Freundlich	N	1.65961
	K_F	0.03084
	R^2	0.94415
Temkin	b	60209.4
	K_b	2.71818
	R^2	0.82183

The results above show that the Langmuir isotherm model had a perfect linear plot with R^2=0.9947 compared to the Freundlich whose R^2 value of 0.94415, and Temkin had a R^2 value of 0.82183. This confirms that the monolayer folic acid is functionalized on the Fe_3O_4 NPs. The results show a similar pattern to the already published work by (Nyirenda et al., 2022, Singogo, 2022). From the plot above the Langmuir isotherm provides a better fit to this experimental data as was also observed by (Castillo et al., 2015) than the Freundlich and Temkin isotherm.

5.7 Drug release profile

5.7.1 Effect of pH on Drug release

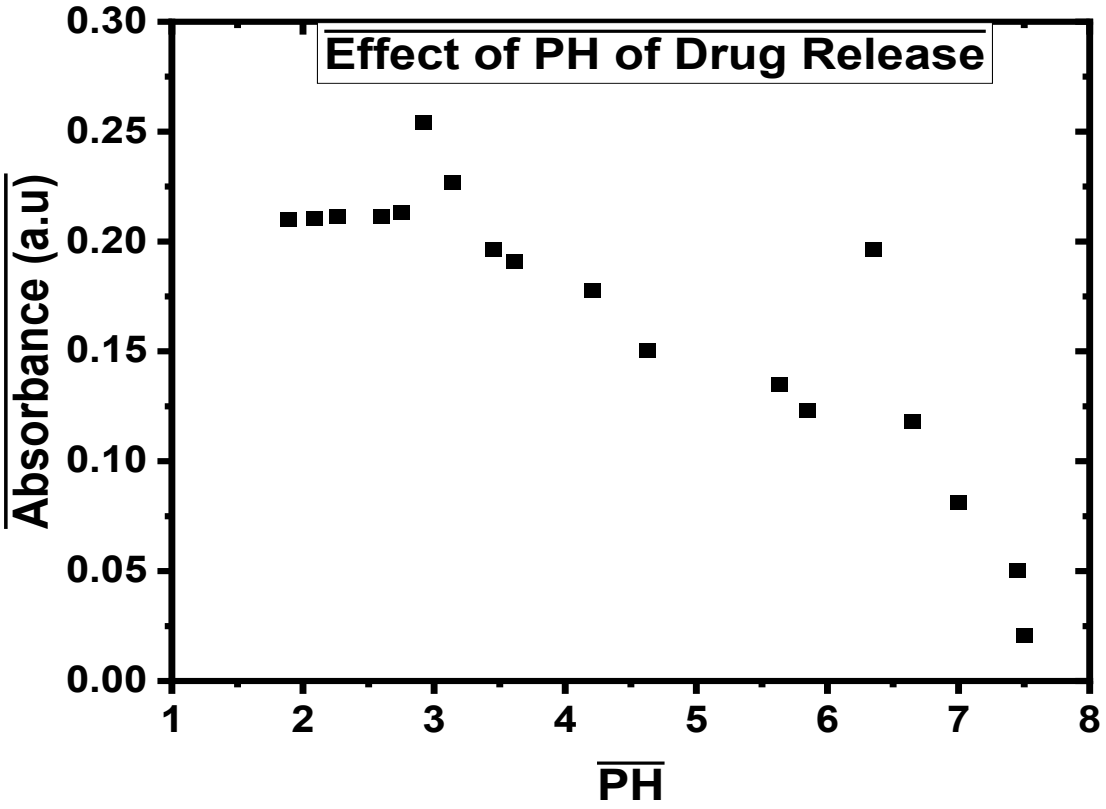

Figure 9: The Effect of pH on Drug Release

The results in Figure 9 show an inverse relationship between pH and Absorbance. Maximum absorbance was observed at a pH of 2.92. These results show that a reduction in pH increases drug concentration, which suggests that DXL is likely to accumulate more in cancer cells microenvironment that have an acidic pH compared to the normal ones (Du et al., 2015). This experiment provides very useful information important in understanding the behaviour of the designed DXL nano delivery system.

5.7.2 Drug Release Studies of Docetaxel

The release of Docetaxel was studied at four different pH, 7.45 (representing the physiological pH), pH 7.0, 6.0, and 4.80 (mimicking the pH of most cancer cells) at 37°C for 72 hr in Phosphate Buffer Solution (PBS). As can be seen in Figure 10, illustrates the release profile of Docetaxel from PEGylated nanoparticles at various pH levels (4.80, 6.0, 7.0, and 7.45) for 72 hr. The

release of Docetaxel is pH-dependent, with the highest release observed at pH 4.80 (approximately 63% after 72 hr) and the lowest at pH 7.45 (around 24% after 72 hr) The release profiles at pH 6.0 and 7.0 fall between these two extremes, with approximately 38% and 28% release after 72 hr respectively. This profile is comprised of two sections; in the first section, a significant drug release of around 40% for pH = 4.8, 21% for 6.0, pH 7.0 with 15%, and pH = 7.4 at 9% was observed from the beginning of the test up to the first 8 hr. In the second section, more sustained drug release was observed in the time interval of 8 to 72 hr and reached 62.4%. 37.8%, 28.3%, and 24.0 %, which were related to pH 4.8, 7.0, 6.0, and pH 7.45, respectively. It seems that in the first time interval, a high drug release rate could be due to the rapid diffusion of Docetaxel due to the increased concentration gradient. In the second section, drug release was found to be uniform with a slow rate and relatively stable; this could be attributed to the steady state and the stability of the delivery system due to PEG Folic Acid. Studies have consistently shown that the release of drugs from nanoparticles can be influenced by the pH of the surrounding environment. For instance, Yang investigated the release of Doxorubicin from pH-sensitive nanoparticles and observed a similar pH-dependent release profile, with increased release at lower pH values (Yang et al., 2019a). In another study Levit examined the release of Paclitaxel from PEGylated nanoparticles and found that the release was influenced by the pH of the release medium, with faster release at lower pH values (Levit et al., 2020).

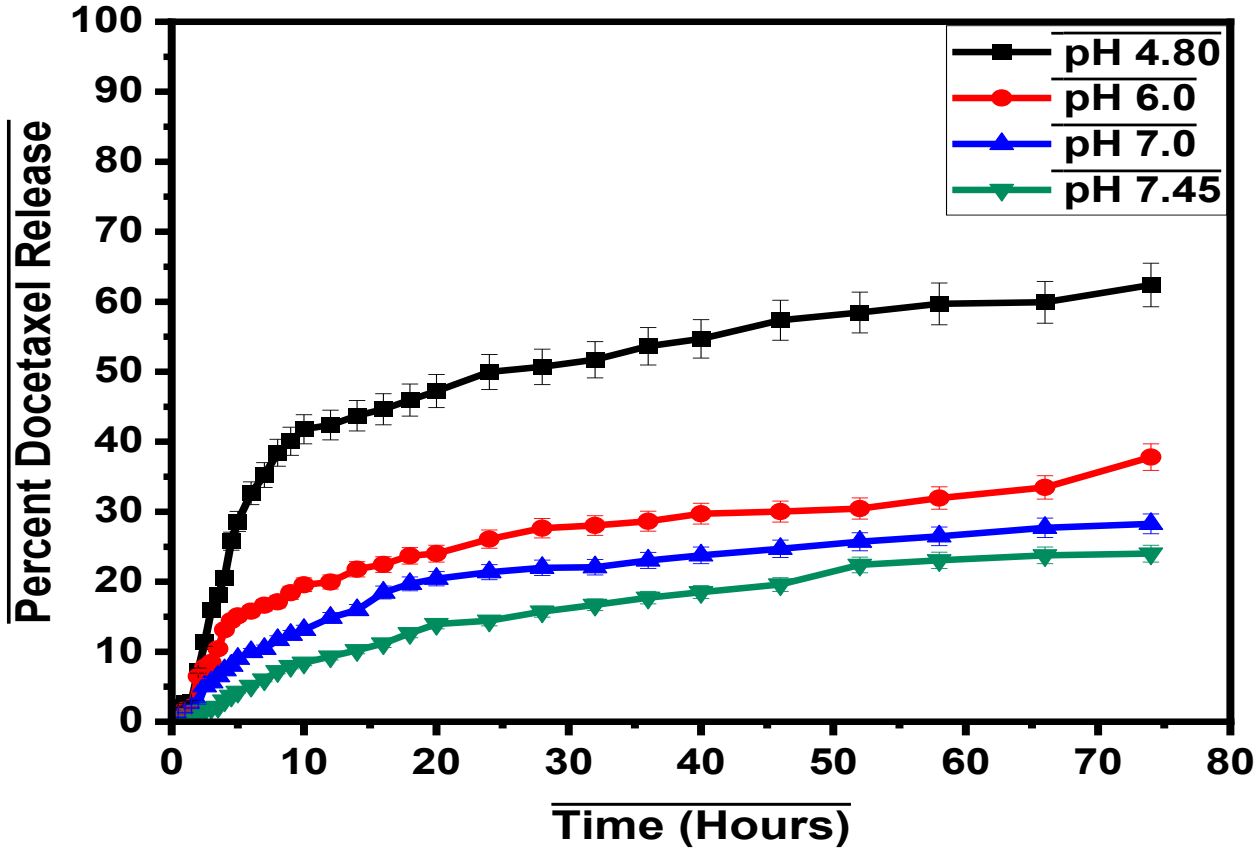

Figure 10: Docetaxel drug release of PEGylated Nanoparticles at pH 4.80, pH 6.0, pH 7.0 and pH 7.45.

It is worth noting that in figure 10 there is a considerable percentage difference between Docetaxel at pH 4.8 and pH 7.45 within the same period. Cancer cells have a more acidic microenvironment compared to normal cells and as such this designed drug delivery system is likely to release more Docetaxel around the cancer cell, as was observed. Drug release was faster, pH 4.8 (63%) while 38% at pH 7.45 after 72 hr. This reveals that pH affects hydrolysis of the ester linkage, that is, at acidic pH, hydrolysis if the bond is faster than at neutral or slightly basic. Our results are comparable to previous reports (Wei et al., 2017). As can be seen in figure 10, the DXL drug release was controlled in this system such that 62.4% of the total loaded drug was released continuously and sustainably within 72 hr.

Overall, the pH-dependent release of Docetaxel from PEGylated nanoparticles shown above has significant implications for cancer therapy, as the tumor microenvironment is often characterized by a lower pH compared to normal tissues. This property can be exploited to achieve targeted drug delivery, where the nanoparticles release the drug more rapidly in the acidic tumor environment, thereby enhancing therapeutic efficacy and reducing side effects (Adepu and Ramakrishna, 2021).

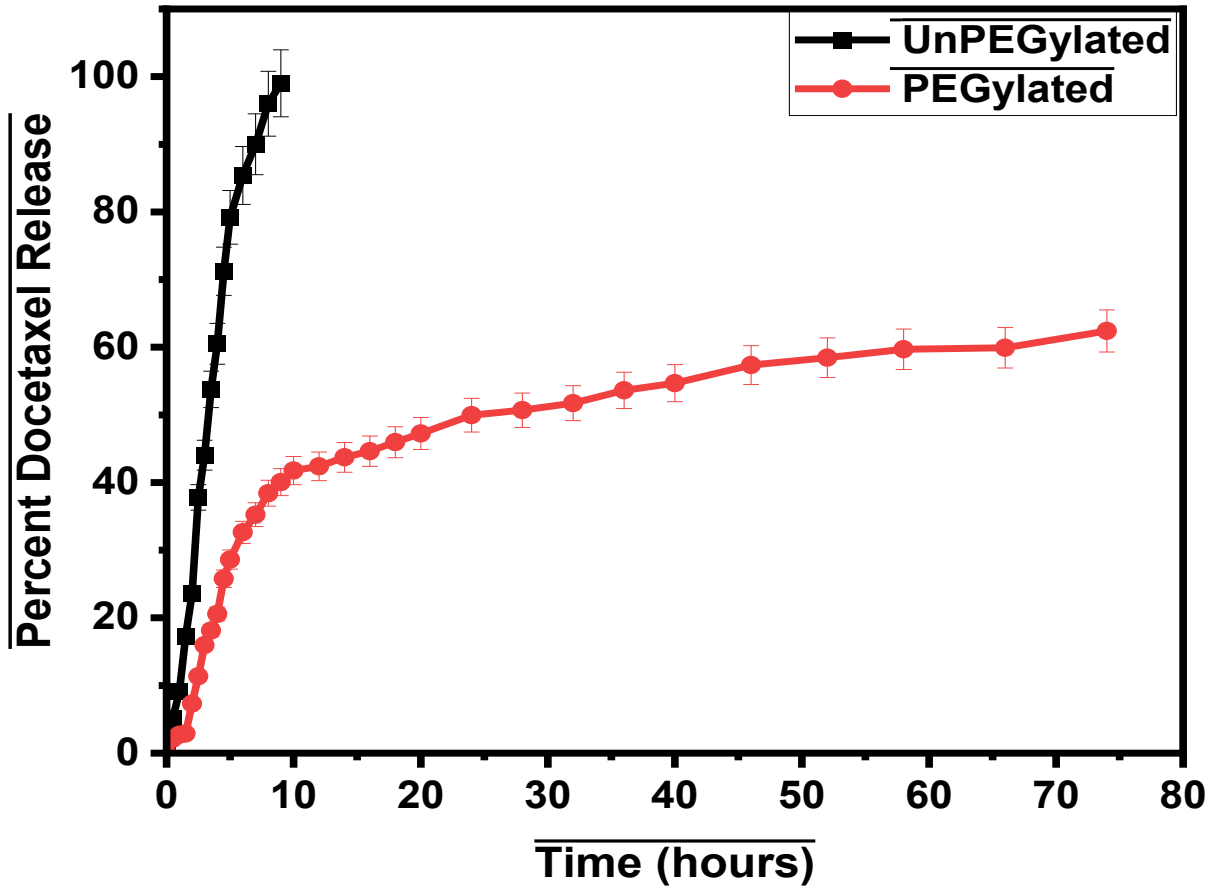

Figure 11: Docetaxel release of PEGylated and UnPEGylated Nanoparticles at pH 4.80.

Figure 11 illustrates the release profile of docetaxel, a chemotherapy medication, from two different formulations: unPegylated (Fe_3O_4@FA@DXL) and PEGylated (Fe_3O_4@FA@DXL@PEG. The data reveals that the unPEGylated formulation exhibits a rapid release of docetaxel, reaching 99% release within approximately 8 hr. In contrast, the PEGylated formulation demonstrates a more controlled release, with a slower initial release rate and a maximum release of around 63% over 72 hr. The developed drug delivery system) was able to sustain the drug release over 72 hr; however, the free drug was released in 8 hr. The results vouch for the sustained and controlled drug release behaviour of the developed drug delivery system, proving that PEGylation improved the stability of the delivery system. These results are comparable to (Liu et al., 2016, Ebadi et al., 2023). Our results confirm that PEG stabilizes drug-loaded nanoparticles and increases circulation time. Various Studies have consistently shown that PEGylation can modify the release characteristics of drugs from nanoparticles. For instance, research on PEGylated nanoparticles has demonstrated improved circulation times and reduced clearance rates, resulting in more sustained drug release profiles (Suk et al., 2016, Santhanakrishnan et al., 2024).

5.7.3. Drug Release Kinetics

Different mathematical models were used to understand the drug release kinetics. The model used includes zero, first, and second order, the Higuchi, and the Korsmeyer-Peppas model (Paarakh et al., 2018). Table 3 below shows the data used to develop linear plots of the

Table 3: Variables for the Kinetics Models

Time	Cumulative DXL Release (pH 4.80)	Zero order	First order	Second Order	Higuchi	Korsmeyer-Peppas
Min	%	[A]t	ln[A]t	1/[A]t	Square root(t)	log mt/m
420	35.2	35.24	3.5622	0.02838	20.4939	1.5470
480	38.4	38.42	3.6486	0.02603	21.9089	1.5846
540	40.1	40.06	3.6904	0.02496	23.2379	1.6027
600	41.8	41.78	3.7324	0.02393	24.4949	1.6210
720	42.4	42.4	3.7471	0.02358	26.8328	1.6274
840	43.7	43.72	3.7778	0.02287	28.9828	1.6407
960	44.6	44.64	3.7986	0.02240	30.9839	1.6497
1080	46.0	45.96	3.8278	0.02176	32.8634	1.6624
1200	47.2	47.24	3.8552	0.02117	34.6410	1.6743
1440	50.0	49.96	3.9112	0.02002	37.9473	1.6986
1680	50.7	50.7	3.9259	0.01972	40.9878	1.7050
1920	51.7	51.72	3.9458	0.01933	43.8178	1.7137
2160	53.6	53.64	3.9823	0.01864	46.4758	1.7295
2400	54.7	54.7	4.0019	0.01828	48.9898	1.7380
2760	57.4	57.36	4.0493	0.01743	52.5357	1.7586
3120	58.5	58.46	4.0683	0.01711	55.8570	1.7669
3480	59.7	59.7	4.0893	0.01675	58.9915	1.7760
3960	59.9	59.92	4.0930	0.01669	62.9285	1.7776
4440	62.4	62.4	4.1336	0.01603	66.6333	1.7952

The table above shows part of the drug release profile, where the drug release was steady, because when studying drug release kinetics, it's crucial to select the appropriate model and determine the valid segment of the release profile for that model (Jahromi et al., 2020).

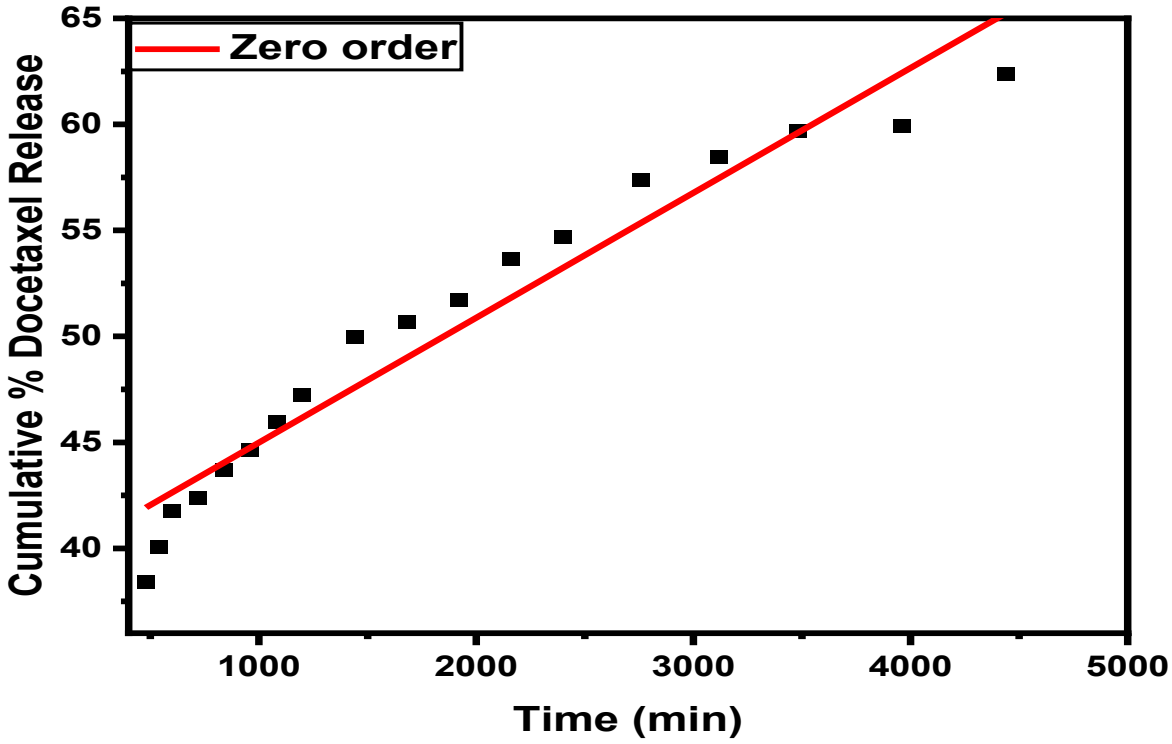

Figure 12: Zero-order drug release kinetic model plot

The linear plot for the Zero-order drug release kinetic model plot and corresponding R-squared values was R^2=0.91221. the R^2 value shows a great deviation from a perfect linear plot.

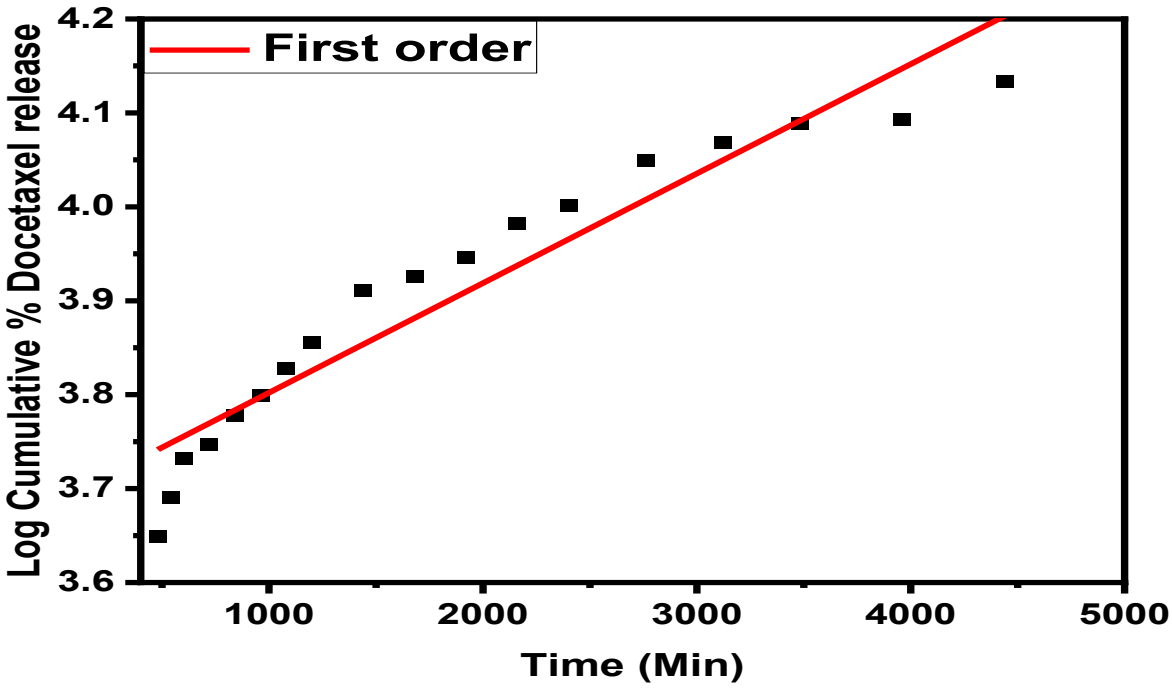

Figure 13: First-order drug release kinetic model plot

The linear plot for the first-order drug release kinetic model plot and corresponding R-squared values was R^2=0.90668, the R^2 value is lower than the zero order.

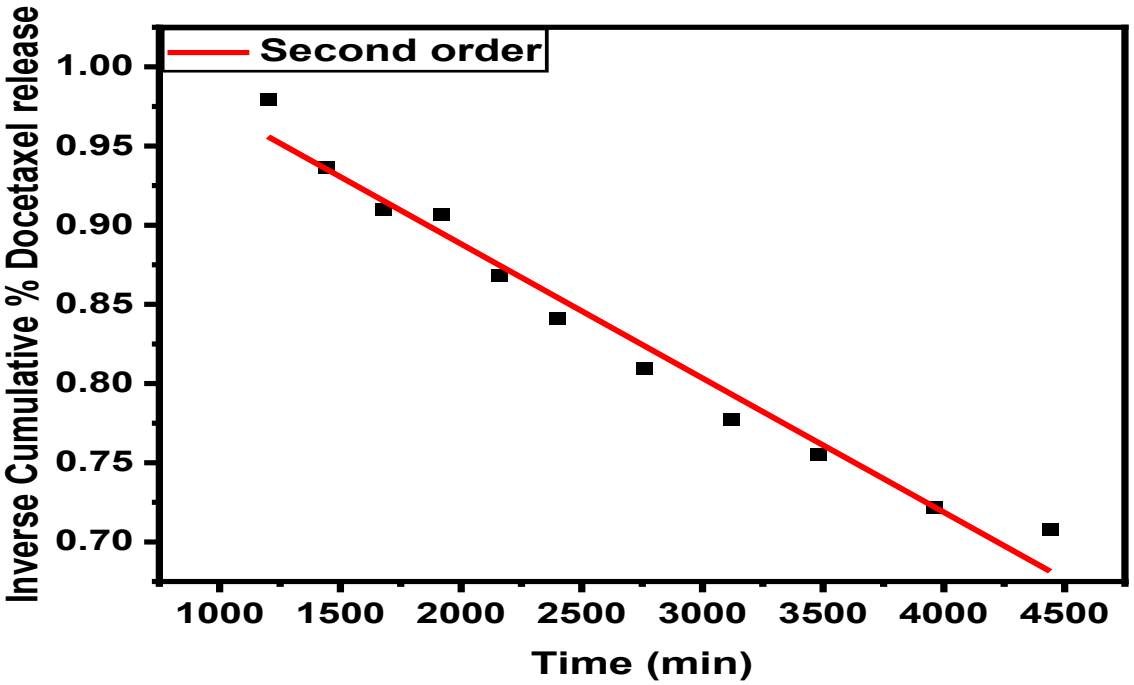

Figure 14: Second-order drug release kinetic model plot

The linear plot for the second-order (figure 14) drug release kinetic model plot and corresponding R-squared values were 0.97414. This shows better linearity.

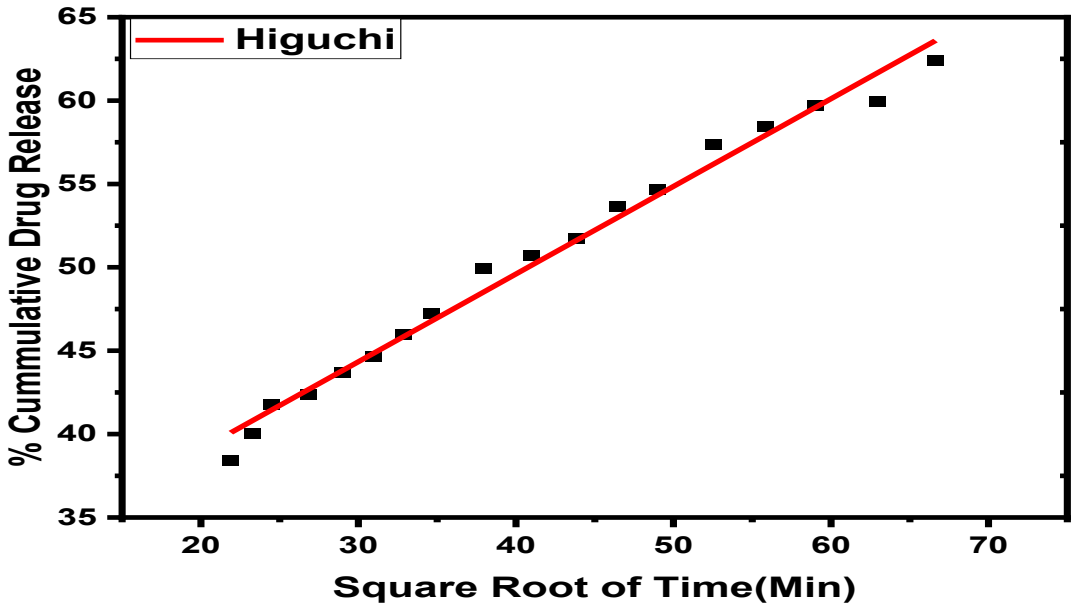

Figure 15: Higuchi drug release kinetic model plot

The linear plot for the Higuchi kinetic model plot with R^2=0.98679, which provides a better fit.

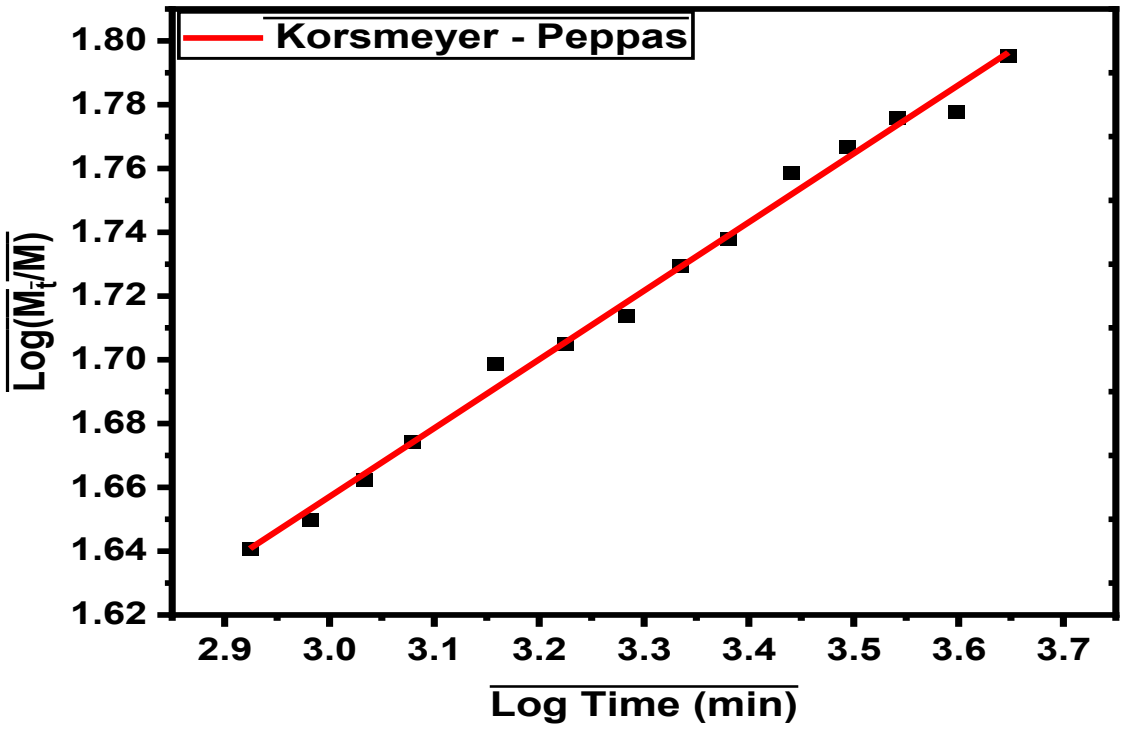

Figure 16: Korsmeyer - Peppas drug release kinetic model plot

The linear plot for the Korsmeyer–Peppas drug release kinetic model plot and the corresponding R-squared value of 0.9949. of the five kinetic models used, our findings show that drug release follows the Korsmeyer–Peppas kinetics and Fickian diffusion release mechanism, since the n value was less than 0.43 and dissolution (Permanadewi et al., 2019). Considering the R-squared values for the examined model, the Korsmeyer–Peppas kinetic model gives a more linear plot, proposing that the drug release of the designed delivery systems follows this model.

In the present research iron oxide nanoparticles can be synthesised by co-precipitation of ferric and ferrous iron. The reproducibility of this work largely depends on maintaining the correct ratio of Fe^{3+}: Fe^{2+} of 2:1 and pH of 9.2. Functionalisation depends on the subsequent experiment and desired functional groups. It is important to use a compound with bifunctional groups. Short time intervals are advised at the beginning of the drug release experiment and then proceeding with a new time interval when a slow release is observed. Mathematical kinetic models must be used with an understanding of the region of the drug release profile that

gives a better fit and reproducible results. This work provides more insights into developing smart drug delivery systems by elucidating the drug release kinetics and showing the effect of pH and PEGylation on drug release mechanism and kinetics.

Chapter Six

Conclusion And Recommendations

6.1 Conclusion

This present work has demonstrated that Docetaxel-loaded pegylated magnetic nanoparticles were designed, synthesized and characterized. This was verified by UV-Vis, XRD, and FT-IR results and was consistent with previous reports (Pourjavadi et al., 2016, Wei et al., 2017, Singogo, 2022, Ebadi et al., 2023). The pH of the environment played a crucial role in drug release from pegylated nanoparticles. At pH 4.8, DXL release was faster, recording 62.4%, while at pH 7.45, drug release was 37.8% after 72 hr. This shows that this system would release more DXL in the prostate cancer microenvironment than in normal cells. This differential drug release has the potential to reduce side effects in current DXL administration methods. The pegylated nanoparticles exhibited a sustained release pattern, unlike unPegylated ones, the results prove that PEG stabilises Docetaxel-loaded nanoparticles and increases circulation time. The drug release kinetics were aligned to the Korsmeyer-Peppas release model with a R^2 = 0.99490 (Zaman et al., 2022). The Korsmeyer-Peppas release exponent $n < 0.43$, suggest that the Fickian diffusion release mechanism is followed (Permanadewi et al., 2019, Telsang et al., 2022). Overall, this work provides more insights into developing smart drug delivery systems by elucidating the drug release kinetics.

6.2 Recommendations

This work has shown that Docetaxel-loaded PEGylated Fe_3O_4 NPs have sustained release in vitro studies following the Korsmeyer – Peppas kinetic model. Further work needs to be done that focuses on exploring and interrogating the application of the Korsmeyer – Peppas to optimize the design and drug release using different types of Encapsulating agents. In Vivo studies are also recommended, as well as toxicity studies to establish the safety of the developed drug PEGylated Docetaxel-loaded Fe_3O_4NPs both in normal and prostate cancer cells.

References

ADEPU, S. & RAMAKRISHNA, S. 2021. Controlled drug delivery systems: current status and future directions. *Molecules,* 26**,** 5905.

AGGARWAL, R., HUANG, J., ALUMKAL, J. J., ZHANG, L., FENG, F. Y., THOMAS, G. V., WEINSTEIN, A. S., FRIEDL, V., ZHANG, C. & WITTE, O. N. 2018. Clinical and genomic characterization of treatment-emergent small-cell neuroendocrine prostate cancer: a multi-institutional prospective study. *Journal of Clinical Oncology,* 36**,** 2492.

AL SAQR, A., WANI, S. U. D., GANGADHARAPPA, H., ALDAWSARI, M. F., KHAFAGY, E.-S. & LILA, A. S. A. 2021. Enhanced cytotoxic activity of docetaxel-loaded silk fibroin nanoparticles against breast cancer cells. *Polymers,* 13**,** 1416.

ALI, A., ALSALHI, M., ATIF, M., ANSARI, A. A., ISRAR, M. Q., SADAF, J., AHMED, E., NUR, O. & WILLANDER, M. Potentiometric urea biosensor utilizing nanobiocomposite of chitosan-iron oxide magnetic nanoparticles. Journal of Physics: Conference Series, 2013. IOP Publishing, 012024.

ALKEN, S. & KELLY, C. M. 2013. Benefit risk assessment and update on the use of docetaxel in the management of breast cancer. *Cancer Management and Research***,** 357-365.

ANCIRA-CORTEZ, A., MORALES-AVILA, E., OCAMPO-GARCÍA, B. E., GONZÁLEZ-ROMERO, C., MEDINA, L. A., LÓPEZ-TÉLLEZ, G. & CUEVAS-YÁÑEZ, E. 2017a. Preparation and characterization of a tumor-targeting dual-image system based on iron oxide nanoparticles functionalized with folic acid and rhodamine. *Journal of Nanomaterials,* 2017(1), p.5184167.

ANCIRA-CORTEZ, A., MORALES-AVILA, E., OCAMPO-GARCÍA, B. E., GONZÁLEZ-ROMERO, C., MEDINA, L. A., LÓPEZ-TÉLLEZ, G. & CUEVAS-YÁÑEZ, E. 2017b. Preparation and Characterization of a Tumor-Targeting Dual-Image System Based on Iron Oxide Nanoparticles Functionalized with Folic Acid and Rhodamine. *Journal of Nanomaterials,* 2017**,** 5184167.

ANSARI, S. A. M. K., FICIARÀ, E., RUFFINATTI, F. A., STURA, I., ARGENZIANO, M., ABOLLINO, O., CAVALLI, R., GUIOT, C. & D'AGATA, F. 2019. Magnetic iron oxide nanoparticles: synthesis, characterization and functionalization for biomedical applications in the central nervous system. *Materials,* 12**,** 465.

ATTIA, N. F., ABD EL-MONAEM, E. M., EL-AQAPA, H. G., ELASHERY, S. E., ELTAWEIL, A. S., EL KADY, M., KHALIFA, S. A., HAWASH, H. B. & EL-SEEDI,

H. R. 2022. Iron oxide nanoparticles and their pharmaceutical applications. *Applied Surface Science Advances,* 11**,** 100284.

BAEK, J.-S. & CHO, C.-W. 2015. Comparison of solid lipid nanoparticles for encapsulating paclitaxel or docetaxel. *Journal of pharmaceutical investigation,* 45**,** 625-631.

BAI, X., SMITH, Z. L., WANG, Y., BUTTERWORTH, S. & TIRELLA, A. 2022. Sustained drug release from smart nanoparticles in cancer therapy: A Comprehensive review. *Micromachines,* 13**,** 1623.

BANERJEE, A., QI, J., GOGOI, R., WONG, J. & MITRAGOTRI, S. 2016. Role of nanoparticle size, shape and surface chemistry in oral drug delivery. *Journal of Controlled Release,* 238**,** 176-185.

BANIK, B. K. 2020. *Green Approaches in Medicinal Chemistry for Sustainable Drug Design*: *Applications* (Vol. 1). Elsevier.

BAŞ, E. & NAZıROĞLU, M. 2019. Treatment with melatonin and selenium attenuates docetaxel-induced apoptosis and oxidative injury in kidney and testes of mice. *Andrologia,* 51**,** e13320.

BEKALU, Y. E., WUDU, M. A. & GASHU, A. W. 2023. Adherence to Chemotherapy and Associated Factors Among Patients With Cancer in Amhara Region, Northeastern Ethiopia, 2022. A Cross-Sectional Study. *Cancer Control,* 30**,** 10732748231185010.

BRAY, F., LAVERSANNE, M., SUNG, H., FERLAY, J., SIEGEL, R. L., SOERJOMATARAM, I. & JEMAL, A. 2024. Global cancer statistics 2022: GLOBOCAN estimates of incidence and mortality worldwide for 36 cancers in 185 countries. *CA: a cancer journal for clinicians,* 74**,** 229-263.

BROWN, S. B., WANG, L., JUNGELS, R. R. & SHARMA, B. 2020. Effects of cartilage-targeting moieties on nanoparticle biodistribution in healthy and osteoarthritic joints. *Acta biomaterialia,* 101**,** 469-483.

CARVALHO, P. M., FELÍCIO, M. R., SANTOS, N. C., GONÇALVES, S. & DOMINGUES, M. M. 2018. Application of light scattering techniques to nanoparticle characterization and development. *Frontiers in chemistry,* 6**,** 237.

CASTILLO, J. J., RINDZEVICIUS, T., ROZO, C. E. & BOISEN, A. 2015. Adsorption and vibrational study of folic acid on gold nanopillar structures using surface-enhanced Raman scattering spectroscopy. *Nanomaterials and nanotechnology,* 5**,** 29.

CHEN, Q., LIU, D., WU, C., YAO, K., LI, Z., SHI, N., WEN, F. & GATES, I. D. 2018. Co-immobilization of cellulase and lysozyme on amino-functionalized magnetic

nanoparticles: an activity-tunable biocatalyst for extraction of lipids from microalgae. *Bioresource technology,* 263**,** 317-324.

CHENG, Z., LI, M., DEY, R. & CHEN, Y. 2021. Nanomaterials for cancer therapy: current progress and perspectives. *Journal of hematology & oncology,* 14**,** 1-27.

CONG, Z., SHI, Y., WANG, Y., WANG, Y., CHEN, N. & XUE, H. 2018. A novel controlled drug delivery system based on alginate hydrogel/chitosan micelle composites. *International journal of biological macromolecules,* 107**,** 855-864.

DADSETAN, M., TAYLOR, K. E., YONG, C., BAJZER, Ž., LU, L. & YASZEMSKI, M. J. 2013. Controlled release of doxorubicin from pH-responsive microgels. *Acta biomaterialia,* 9**,** 5438-5446.

DANG, Y. & GUAN, J. 2020. Nanoparticle-based drug delivery systems for cancer therapy. *Smart materials in medicine,* 1**,** 10-19.

DASH, S., MURTHY, P. N., NATH, L. & CHOWDHURY, P. 2010. Kinetic modeling on drug release from controlled drug delivery systems. *Acta Pol Pharm,* 67**,** 217-223.

DAY, C. M., SWEETMAN, M. J., SONG, Y., PLUSH, S. E. & GARG, S. 2021. Functionalized mesoporous silica nanoparticles as Delivery Systems for Doxorubicin: Drug loading and Release. *Applied Sciences,* 11**,** 6121.

DE OLIVEIRA, R., ZHAO, P., LI, N., DE SANTA MARIA, L. C., VERGNAUD, J., RUIZ, J., ASTRUC, D. & BARRATT, G. 2013. Synthesis and in vitro studies of gold nanoparticles loaded with docetaxel. *International journal of pharmaceutics,* 454**,** 703-711.

DEBELA, D. T., MUZAZU, S. G., HERARO, K. D., NDALAMA, M. T., MESELE, B. W., HAILE, D. C., KITUI, S. K. & MANYAZEWAL, T. 2021. New approaches and procedures for cancer treatment: Current perspectives. *SAGE open medicine,* 9**,** 20503121211034366.

DONBROW, M. & FRIEDMAN, M. 1975. Timed release from polymeric films containing drugs and kinetics of drug release. *Journal of pharmaceutical sciences,* 64**,** 76-80.

DU, J., LANE, L. A. & NIE, S. 2015. Stimuli-responsive nanoparticles for targeting the tumor microenvironment. *Journal of Controlled Release,* 219**,** 205-214.

EBADI, M., RIFQI MD ZAIN, A., TENGKU ABDUL AZIZ, T. H., MOHAMMADI, H., TEE, C. A. T. & RAHIMI YUSOP, M. 2023. Formulation and characterization of Fe_3O_4@ PEG nanoparticles loaded sorafenib; molecular studies and evaluation of cytotoxicity in liver cancer cell lines. *Polymers,* 15**,** 971.

ESLAMI, P., ALBINO, M., SCAVONE, F., CHIELLINI, F., MORELLI, A., BALDI, G., CAPPIELLO, L., DOUMETT, S., LORENZI, G. & RAVAGLI, C. 2022. Smart magnetic nanocarriers for multi-stimuli on-demand drug delivery. *Nanomaterials,* 12**,** 303.

FASIKU, V., AMUHAYA, E. K., RAJAB, K. M. & OMOLO, C. A. 2020. Nano/microparticles encapsulation via covalent drug conjugation. *Nano-and Microencapsulation-Techniques and Applications.* IntechOpen.

FENTON, O. S., OLAFSON, K. N., PILLAI, P. S., MITCHELL, M. J. & LANGER, R. 2018. Advances in biomaterials for drug delivery. *Advanced Materials,* 30**,** 1705328.

FERLAY, J., ERVIK, M., LAM, F., LAVERSANNE, M., COLOMBET, M., MERY, L., PIÑEROS, M., ZNAOR, A., SOERJOMATARAM, I. & BRAY, F. 2024. Global cancer observatory: cancer today (version 1.1). Lyon, France: International Agency for Research on Cancer; 2024.

FERNANDES, A. I. 2023. Polymers enhancing bioavailability in drug delivery. MDPI.

FONSECA-SANTOS, B., GREMIÃO, M. P. D. & CHORILLI, M. 2015. Nanotechnology-based drug delivery systems for the treatment of Alzheimer's disease. *International Journal of nanomedicine***,** 4981-5003.

GAO, Y., GAO, D., SHEN, J. & WANG, Q. 2020. A review of mesoporous silica nanoparticle delivery systems in chemo-based combination cancer therapies. *Frontiers in chemistry,* 8**,** 598722.

GOKHALE, A. 2014. Achieving zero-order release kinetics using multi-step diffusion-based drug delivery. *Pharmaceutical Technology,* 38.

GUO, K., XIAO, N., LIU, Y., WANG, Z., TÓTH, J., GYENIS, J., THAKUR, V. K., OYANE, A. & SHUBHRA, Q. T. 2022. Engineering polymer nanoparticles using cell membrane coating technology and their application in cancer treatments: Opportunities and challenges. *Nano Materials Science,* 4**,** 295-321.

GUPTA, P. & PURWAR, R. 2021. Influence of cross-linkers on the properties of cotton grafted poly (acrylamide-co-acrylic acid) hydrogel composite: Swelling and drug release kinetics. *Iranian Polymer Journal,* 30**,** 381-391.

HAMEDANI, S. & FELRGARI, Z. 2017. Adsorption properties of folic acid onto functionalized carbon nanotubes: isotherms and thermodynamics studies. *Physical Chemistry Research,* 5**,** 519-529.

HAO, G., XU, Z. P. & LI, L. 2018. Manipulating extracellular tumour pH: An effective target for cancer therapy. *RSC advances,* 8**,** 22182-22192.

HERDIANA, Y., FEBRINA, E., NURHASANAH, S., GOZALI, D., ELAMIN, K. M. & WATHONI, N. 2024. Drug loading in chitosan-based nanoparticles. *Pharmaceutics,* 16**,** 1043.

HERDIANA, Y., WATHONI, N., SHAMSUDDIN, S. & MUCHTARIDI, M. 2022. Drug release study of the chitosan-based nanoparticles. *Heliyon*.

HO, M. Y. & MACKEY, J. R. 2014. Presentation and management of docetaxel-related adverse effects in patients with breast cancer. *Cancer management and research***,** 253-259.

HU, C.-M. J., ZHANG, L., ARYAL, S., CHEUNG, C., FANG, R. H. & ZHANG, L. 2011. Erythrocyte membrane-camouflaged polymeric nanoparticles as a biomimetic delivery platform. *Proceedings of the National Academy of Sciences,* 108**,** 10980-10985.

HUA, H., ZHANG, N., LIU, D., SONG, L., LIU, T., LI, S. & ZHAO, Y. 2017. Multifunctional gold nanorods and docetaxel-encapsulated liposomes for combined thermo-and chemotherapy. *International journal of nanomedicine***,** 7869-7884.

JAHROMI, L. P., GHAZALI, M., ASHRAFI, H. & AZADI, A. 2020. A comparison of models for the analysis of the kinetics of drug release from PLGA-based nanoparticles. *Heliyon,* 6.

JALILIAN, A., HOSSEINI-SALEKDEH, S., MAHMOUDI, M., YOUSEFNIA, H., MAJDABADI, A. & POULADIAN, M. 2011. Preparation and biological evaluation of radiolabeled-folate embedded superparamagnetic nanoparticles in wild-type rats. *Journal of Radioanalytical and Nuclear Chemistry,* 287**,** 119-127.

KALAM, M. A., HUMAYUN, M., PARVEZ, N., YADAV, S., GARG, A., AMIN, S., SULTANA, Y. & ALI, A. 2007. Release kinetics of modified pharmaceutical dosage forms: a review. *Cont. J. Pharm. Sci,* 1**,** 30-35.

KHALID, A., PERSANO, S., SHEN, H., ZHAO, Y., BLANCO, E., FERRARI, M. & WOLFRAM, J. 2017. Strategies for improving drug delivery: nanocarriers and microenvironmental priming. *Expert opinion on drug delivery,* 14**,** 865-877.

KRAUS, L. A., SAMUEL, S. K., SCHMID, S. M., DYKES, D. J., WAUD, W. R. & BISSERY, M. C. 2003. The mechanism of action of docetaxel (Taxotere®) in xenograft models is not limited to bcl-2 phosphorylation. *Investigational new drugs,* 21**,** 259-268.

LARACUENTE, M.-L., MARINA, H. Y. & MCHUGH, K. J. 2020. Zero-order drug delivery: State of the art and future prospects. *Journal of Controlled Release,* 327**,** 834-856.

LAZARO-CARRILLO, A., FILICE, M., GUILLÉN, M. J., AMARO, R., VIÑAMBRES, M., TABERO, A., PAREDES, K. O., VILLANUEVA, A., CALVO, P. & DEL PUERTO MORALES, M. 2020. Tailor-made PEG coated iron oxide nanoparticles as contrast agents for long lasting magnetic resonance molecular imaging of solid cancers. *Materials Science and Engineering: C,* 107**,** 110262.

LE, Z., CHEN, Y., HAN, H., TIAN, H., ZHAO, P., YANG, C., HE, Z., LIU, L., LEONG, K. W. & MAO, H.-Q. 2018. Hydrogen-bonded tannic acid-based anticancer nanoparticle for enhancement of oral chemotherapy. *ACS applied materials & interfaces,* 10**,** 42186-42197.

LEVIT, S. L., GADE, N. R., ROPER, T. D., YANG, H. & TANG, C. 2020. Self-assembly of ph-labile polymer nanoparticles for paclitaxel prodrug delivery: Formulation, characterization, and evaluation. *International Journal of Molecular Sciences,* 21**,** 9292.

LI, Q., XIONG, Y., JI, C. & YAN, Z. 2019. The application of nanotechnology in the codelivery of active constituents of plants and chemotherapeutics for overcoming physiological barriers during antitumor treatment. *BioMed Research International,* 2019.

LIMA, T. S., IGLESIAS-GATO, D., SOUZA, L. D., STENVANG, J., LIMA, D. S., RØDER, M. A., BRASSO, K. & MOREIRA, J. M. 2021. Molecular profiling of docetaxel-resistant prostate cancer cells identifies multiple mechanisms of therapeutic resistance. *Cancers,* 13**,** 1290.

LIU, B., WANG, Y., YU, Q., LI, D. & LI, F. 2018. Synthesis, characterization of catechin-loaded folate-conjugated chitosan nanoparticles and their anti-proliferative effect. *CyTA-Journal of Food,* 16**,** 868-876.

LIU, F., SUN, Y., KANG, C. & ZHU, H. 2016. Pegylated drug delivery systems: from design to biomedical applications. *Nano Life,* 6**,** 1642002.

LIU, J. F., JANG, B., ISSADORE, D. & TSOURKAS, A. 2019. Use of magnetic fields and nanoparticles to trigger drug release and improve tumor targeting. *Wiley Interdisciplinary Reviews: Nanomedicine and Nanobiotechnology,* 11**,** e1571.

LOURENÇO, I., PELEGRINO, M., PIERETTI, J., ANDRADE, G., CERCHIARO, G. & SEABRA, A. Synthesis, characterization and cytotoxicity of chitosan-coated Fe3O4

nanoparticles functionalized with ascorbic acid for biomedical applications. Journal of Physics: Conference Series, 2019. IOP Publishing, 012015.

MARKOWSKI, M. C. & CARDUCCI, M. A. 2017. Early use of chemotherapy in metastatic prostate cancer. *Cancer treatment reviews,* 55**,** 218-224.

MCCARTHY, C., AHERN, R., DEVINE, K. & CREAN, A. 2017. Role of Drug Adsorption onto the Silica Surface in Drug Release from Mesoporous Silica Systems. *Molecular Pharmaceutics,* 15.

MI, Y., ZHANG, J., TAN, W., MIAO, Q., LI, Q. & GUO, Z. 2022. Preparation of doxorubicin-loaded carboxymethyl-β-cyclodextrin/chitosan nanoparticles with antioxidant, antitumor activities and ph-sensitive release. *Marine Drugs,* 20**,** 278.

MISHRA, A. & SARDAR, M. 2015. Isolation of genomic DNA by silane-modified iron oxide nanoparticles. *Nanotechnology: novel perspectives and prospects. McGraw Hill Education, New York***,** 309-315.

MITCHELL, M. J., BILLINGSLEY, M. M., HALEY, R. M., WECHSLER, M. E., PEPPAS, N. A. & LANGER, R. 2021. Engineering precision nanoparticles for drug delivery. *Nature reviews drug discovery,* 20**,** 101-124.

MONTIEL SCHNEIDER, M. G., MARTÍN, M. J., OTAROLA, J., VAKARELSKA, E., SIMEONOV, V., LASSALLE, V. & NEDYALKOVA, M. 2022. Biomedical applications of iron oxide nanoparticles: current insights progress and perspectives. *Pharmaceutics,* 14**,** 204.

NAZ, S., WANG, M., HAN, Y., HU, B., TENG, L., ZHOU, J., ZHANG, H. & CHEN, J. 2019. Enzyme-responsive mesoporous silica nanoparticles for tumor cells and mitochondria multistage-targeted drug delivery. *International journal of nanomedicine***,** 2533-2542.

NYIRENDA, J., KALABA, G. & MUNYATI, O. 2022. Synthesis and characterization of an activated carbon-supported silver-silica nanocomposite for adsorption of heavy metal ions from water. *Results in engineering,* 15**,** 100553.

PAARAKH, M. P., JOSE, P. A., SETTY, C. & PETERCHRISTOPER, G. 2018. Release kinetics–concepts and applications. *International Journal of Pharmacy Research & Technology (IJPRT),* 8**,** 12-20.

PAPACHRISTOS, A., PATEL, J., VASILEIOU, M. & PATRINOS, G. P. 2023. Dose optimization in oncology drug development: the emerging role of pharmacogenomics, pharmacokinetics, and pharmacodynamics. *Cancers,* 15**,** 3233.

PARK, M.-H., KEUM, C.-G., SONG, J.-Y., KIM, D. & CHO, C.-W. 2014. A novel aqueous parenteral formulation of docetaxel using prodrugs. *International Journal of Pharmaceutics,* 462**,** 1-7.

PATRA, J. K., DAS, G., FRACETO, L. F., CAMPOS, E. V. R., RODRIGUEZ-TORRES, M. D. P., ACOSTA-TORRES, L. S., DIAZ-TORRES, L. A., GRILLO, R., SWAMY, M. K. & SHARMA, S. 2018. Nano based drug delivery systems: recent developments and future prospects. *Journal of nanobiotechnology,* 16**,** 1-33.

PERMANADEWI, I., KUMORO, A., WARDHANI, D. & ARYANTI, N. Modelling of controlled drug release in gastrointestinal tract simulation. Journal of Physics: Conference Series, 2019. IOP Publishing, 012063.

PHAM, S. H., CHOI, Y. & CHOI, J. 2020. Stimuli-responsive nanomaterials for application in antitumor therapy and drug delivery. *Pharmaceutics,* 12**,** 630.

PIENIĄŻEK, A., CZEPAS, J., PIASECKA-ZELGA, J., GWOŹDZIŃSKI, K. & KOCEVA-CHYŁA, A. 2013. Oxidative stress induced in rat liver by anticancer drugs doxorubicin, paclitaxel and docetaxel. *Advances in medical sciences,* 58**,** 104-111.

POURJAVADI, A., TEHRANI, Z. M. & MOGHANAKI, A. A. 2016. Folate-conjugated pH-responsive nanocarrier designed for active tumor targeting and controlled release of gemcitabine. *Pharmaceutical research,* 33**,** 417-432.

RAWLA, P. 2019. Epidemiology of prostate cancer. *World journal of oncology,* 10**,** 63.

REHMAN, Q., AKASH, M. S. H., RASOOL, M. F. & REHMAN, K. 2020. Role of kinetic models in drug stability. *Drug Stability and Chemical Kinetics***,** 155-165.

RIVERO-BUCETA, E., VIDAURRE-AGUT, C., VERA-DONOSO, C. S. D., BENLLOCH, J. M., MORENO-MANZANO, V. & BOTELLA, P. 2019. PSMA-targeted mesoporous silica nanoparticles for selective intracellular delivery of docetaxel in prostate cancer cells. *ACS omega,* 4**,** 1281-1291.

ROSENBLUM, D., JOSHI, N., TAO, W., KARP, J. M. & PEER, D. 2018. Progress and challenges towards targeted delivery of cancer therapeutics. *Nature communications,* 9**,** 1-12.

SACHDEVA, V., MONGA, A., VASHISHT, R., SINGH, D., SINGH, A. & BEDI, N. 2022. Iron Oxide Nanoparticles: The precise strategy for targeted delivery of genes, oligonucleotides and peptides in cancer therapy. *Journal of Drug Delivery Science and Technology,* 74**,** 103585.

SANTHANAKRISHNAN, K. R., KOILPILLAI, J., NARAYANASAMY, D. & SANTHANAKRISHNAN, K. 2024. PEGylation in pharmaceutical development: current status and emerging trends in macromolecular and immunotherapeutic drugs. *Cureus,* 16.

SATO, A., ITCHO, N., ISHIGURO, H., OKAMOTO, D., KOBAYASHI, N., KAWAI, K., KASAI, H., KURIOKA, D., UEMURA, H. & KUBOTA, Y. 2013. Magnetic nanoparticles of Fe3O4 enhance docetaxel-induced prostate cancer cell death. *International journal of nanomedicine***,** 3151-3160.

SCHMID, R., NEFFGEN, N. & LINDÉN, M. 2023. Straightforward adsorption-based formulation of mesoporous silica nanoparticles for drug delivery applications. *Journal of Colloid and Interface Science,* 640**,** 961-974.

SEKINO, Y. & TEISHIMA, J. 2020. Molecular mechanisms of docetaxel resistance in prostate cancer. *Cancer Drug Resistance,* 3**,** 676.

SELVARATHINAM, T. & DHESINGH, R. S. 2022. In-Vitro Evaluation of Folic Acid Capped Gold Nanoformulations for Drug Delivery to Prostate Cancer. *ChemistrySelect,* 7**,** e202200759.

SENAPATI, S., MAHANTA, A. K., KUMAR, S. & MAITI, P. 2018. Controlled drug delivery vehicles for cancer treatment and their performance. *Signal transduction and targeted therapy,* 3**,** 7.

SERCOMBE, L., VEERATI, T., MOHEIMANI, F., WU, S. Y., SOOD, A. K. & HUA, S. 2015. Advances and challenges of liposome assisted drug delivery. *Frontiers in pharmacology,* 6**,** 286.

SHOAIB, M. H., TAZEEN, J., MERCHANT, H. A. & YOUSUF, R. I. 2006. Evaluation of drug release kinetics from ibuprofen matrix tablets using HPMC. *Pakistan journal of pharmaceutical sciences,* 19**,** 119-124.

SINGHVI, G. & SINGH, M. 2011. In-vitro drug release characterization models. *Int J Pharm Stud Res,* 2**,** 77-84.

SINGOGO, R. 2022. *A study of functionalized iron oxide nanoparticles for selective recognition of kappa-casein: a breast cancer biomarker.* The University of Zambia.

SMITH, A. M., DAVE, S., NIE, S., TRUE, L. & GAO, X. 2006. Multicolor quantum dots for molecular diagnostics of cancer. *Expert review of molecular diagnostics,* 6**,** 231-244.

SONG, X., ZHANG, Y., SUN, H., DONG, P., ZHANG, Z. & LIU, J. 2019. In vitro safety evaluation and in vivo imaging studies of superparamagnetic iron oxide nanoparticles through biomimetic modification. *Journal of Nanomaterials,* 2019**,** 1-9.

SOUSA-PIMENTA, M., ESTEVINHO, L. M., SZOPA, A., BASIT, M., KHAN, K., ARMAGHAN, M., IBRAYEVA, M., SÖNMEZ GÜRER, E., CALINA, D. & HANO, C. 2023. Chemotherapeutic properties and side-effects associated with the clinical practice of terpene alkaloids: paclitaxel, docetaxel, and cabazitaxel. *Frontiers in Pharmacology,* 14**,** 1157306.

STOIA, M., ISTRATIE, R. & PĂCURARIU, C. 2016. Investigation of magnetite nanoparticles stability in air by thermal analysis and FTIR spectroscopy. *Journal of Thermal Analysis and Calorimetry,* 125**,** 1185-1198.

SUK, J. S., XU, Q., KIM, N., HANES, J. & ENSIGN, L. M. 2016. PEGylation as a strategy for improving nanoparticle-based drug and gene delivery. *Advanced drug delivery reviews,* 99**,** 28-51.

SUTRADHAR, K. B. & AMIN, M. 2014. Nanotechnology in cancer drug delivery and selective targeting. *International Scholarly Research Notices,* 2014.

TAS, A. & KEKLIKCIOGLU CAKMAK, N. 2021. Synthesis of PEGylated nanographene oxide as a nanocarrier for docetaxel drugs and anticancer activity on prostate cancer cell lines. *Human & Experimental Toxicology,* 40**,** 172-182.

TELSANG, M., PRADEEP, D., WILSON, B., TAMREEN, V., SADIK, S., HABEEBUDDIN, M., ASIF, A. H., ASDAQ, M. B., NAGARAJA, S. H. & NOOR, S. D. 2022. Formulation and Evaluation of Bendamustine Loaded Polymeric Nanoparticle. *Indian Journal of Pharmaceutical Education & Research,* 56.

TEWABE, A., ABATE, A., TAMRIE, M., SEYFU, A. & ABDELA SIRAJ, E. 2021. Targeted drug delivery—from magic bullet to nanomedicine: principles, challenges, and future perspectives. *Journal of Multidisciplinary Healthcare***,** 1711-1724.

THAMBIRAJ, S., SHRUTHI, S., VIJAYALAKSHMI, R. & SHANKARAN, D. R. 2019. Evaluation of cytotoxic activity of docetaxel loaded gold nanoparticles for lung cancer drug delivery. *Cancer Treatment and Research Communications,* 21**,** 100157.

THAMBIRAJ, S., VIJAYALAKSHMI, R. & RAVI SHANKARAN, D. 2021. An effective strategy for development of docetaxel encapsulated gold nanoformulations for treatment of prostate cancer. *Scientific reports,* 11**,** 1-17.

WAGNER, A. M., KNIPE, J. M., ORIVE, G. & PEPPAS, N. A. 2019. Quantum dots in biomedical applications. *Acta biomaterialia,* 94**,** 44-63.

WANG, X., ZHANG, H. & CHEN, X. 2019. Drug resistance and combating drug resistance in cancer. *Cancer Drug Resistance,* 2**,** 141.

WEI, L., LU, B., CUI, L., PENG, X., WU, J., LI, D., LIU, Z. & GUO, X. 2017. Folate-conjugated pH-responsive nanocarrier designed for active tumor targeting and controlled release of doxorubicin. *Frontiers of Materials Science,* 11**,** 328-343.

WEI, Y., HAN, B., HU, X., LIN, Y., WANG, X. & DENG, X. 2012. Synthesis of Fe3O4 nanoparticles and their magnetic properties. *Procedia Engineering,* 27**,** 632-637.

WORSLEY, C. M., VEALE, R. B. & MAYNE, E. S. 2022. The acidic tumour microenvironment: Manipulating the immune response to elicit escape. *Human Immunology,* 83**,** 399-408.

XIA, W., TAO, Z., ZHU, B., ZHANG, W., LIU, C., CHEN, S. & SONG, M. 2021. Targeted delivery of drugs and genes using polymer nanocarriers for cancer therapy. *International Journal of Molecular Sciences,* 22**,** 9118.

XUE, D., LU, H., XU, H. Y., ZHOU, C. X. & HE, X. Z. 2018. Retracted: Long noncoding RNA MALAT 1 enhances the docetaxel resistance of prostate cancer cells via miR-145-5p-mediated regulation of AKAP 12. *Journal of cellular and molecular medicine,* 22**,** 3223-3237.

YANG, J., JIA, C. & YANG, J. 2021. Designing nanoparticle-based drug delivery systems for precision medicine. *International journal of medical sciences,* 18**,** 2943.

YANG, T., DU, G., CUI, Y., YU, R., HUA, C., TIAN, W. & ZHANG, Y. 2019a. pH-sensitive doxorubicin-loaded polymeric nanocomplex based on β-cyclodextrin for liver cancer-targeted therapy. *International Journal of Nanomedicine***,** 1997-2010.

YANG, W., LIANG, H., MA, S., WANG, D. & HUANG, J. 2019b. Gold nanoparticle based photothermal therapy: Development and application for effective cancer treatment. *Sustainable Materials and Technologies,* 22**,** e00109.

YAO, Y., ZHOU, Y., LIU, L., XU, Y., CHEN, Q., WANG, Y., WU, S., DENG, Y., ZHANG, J. & SHAO, A. 2020. Nanoparticle-based drug delivery in cancer therapy and its role in overcoming drug resistance. *Frontiers in molecular biosciences,* 7**,** 193.

YIN, P. T., SHAH, S., CHHOWALLA, M. & LEE, K.-B. 2015. Design, synthesis, and characterization of graphene–nanoparticle hybrid materials for bioapplications. *Chemical reviews,* 115**,** 2483-2531.

ZAMAN, M., BUTT, M. H., SIDDIQUE, W., IQBAL, M. O., NISAR, N., MUMTAZ, A., NAZEER, H. Y., ALSHAMMARI, A. & RIAZ, M. S. 2022. Fabrication of pegylated chitosan nanoparticles containing tenofovir alafenamide: synthesis and characterization. *Molecules,* 27**,** 8401.

ZHANG, C.-X., CHENG, Y., LIU, D.-Z., LIU, M., CUI, H., ZHANG, B.-L., MEI, Q.-B. & ZHOU, S.-Y. 2019. Mitochondria-targeted cyclosporin A delivery system to treat myocardial ischemia reperfusion injury of rats. *Journal of nanobiotechnology,* 17**,** 1-16.

ZHANG, L., BEATTY, A., LU, L., ABDALRAHMAN, A., MAKRIS, T. M., WANG, G. & WANG, Q. 2020. Microfluidic-assisted polymer-protein assembly to fabricate homogeneous functional nanoparticles. *Materials Science and Engineering: C,* 111**,** 110768.

ZHANG, L. & ZHANG, N. 2013. How nanotechnology can enhance docetaxel therapy. *International journal of nanomedicine,* 8**,** 2927.

ZHANG, N., XIONG, G. & LIU, Z. 2022. Toxicity of metal-based nanoparticles: Challenges in the nano era. *Frontiers in Bioengineering and Biotechnology,* 10.

ZHOU, Q., ZHANG, L. & WU, H. 2017. Nanomaterials for cancer therapies. *Nanotechnology Reviews,* 6**,** 473-496.

ZHUANG, J. & KANG, D. 2018. Effect of docetaxel combined with cisplatin chemotherapy with concurrent radiotherapy on short-term prognosis of patients with advanced cervical cancer. *INTERNATIONAL JOURNAL OF CLINICAL AND EXPERIMENTAL MEDICINE,* 11**,** 4898-4904.

ZIELIŃSKA, A., CARREIRÓ, F., OLIVEIRA, A. M., NEVES, A., PIRES, B., VENKATESH, D. N., DURAZZO, A., LUCARINI, M., EDER, P. & SILVA, A. M. 2020. Polymeric nanoparticles: production, characterization, toxicology and ecotoxicology. *Molecules,* 25**,** 3731.

Appendix A-Ethical Clearance

UNIVERSITY OF ZAMBIA
BIOMEDICAL RESEARCH ETHICS COMMITTEE

Telephone: +260977925304
Telegrams: UNZA, LUSAKA
Telex: UNZALU ZA 44370
Fax: + 260-1-250753

Ridgeway Campus
P.O. Box 50110
Lusaka, Zambia
E-mail: unzarec@unza.zm

Federal Assurance No. FWA00000338 IRB00001131 of IORG0000774 NHRAR-REC No 2021-05-0002

28th August 2024

Your REF. No. 5767-2024

Mr. Ian Chisenga,
University of Zambia,
Department of Chemistry,
P.O Box 32379,
Lusaka.

Dear Mr. Chisenga,

RE: ADVANCING PROSTATE CANCER THERAPY: SYNTHESIS AND CHARACTERIZATION OF DOCETAXEL-LOADED MAGNETIC IRON OXIDE NANOPARTICLES FOR CONTROLLED DRUG RELEASE (REF. NO. 5767-2024)

Your application for a waiver of ethics review for the aforementioned study was reviewed. The **waiver** is hereby **granted**. The approval was conducted in line with the University of Zambia Biomedical Research Ethics Committee guidelines on granting waiver of Ethics review.

Date of approval: 26th August 2024 **Date of expiry: 25th August 2025**

CONDITIONS:

- The waiver is based strictly on your submitted proposal. Should there be need for you to modify or make changes to the proposal; you will need to seek clearance from the Biomedical Research Ethics Committee.
- This waiver does not release you from the obligation of ensuring confidentiality.
- If you need any clarifications please consult this office.
- **NHRA:** You are advised to obtain final study clearance and approval to conduct research in Zambia from the National Health Research Authority (NHRA) before commencing the research project.
- **Ensure that a final copy of the results is submitted to this Committee.**

Yours sincerely,

Munsaka.

Prof. Sody Mweetwa Munsaka, BSc., MSc., PhD
CHAIRPERSON